



TECH BRIEFS

NATIONAL AERONAUTICS AND SPACE ADMINISTRATION

-  **Technology Focus**
-  **Computers/Electronics**
-  **Software**
-  **Materials**
-  **Mechanics**
-  **Machinery/Automation**
-  **Manufacturing**
-  **Bio-Medical**
-  **Physical Sciences**
-  **Information Sciences**
-  **Books and Reports**

INTRODUCTION

Tech Briefs are short announcements of innovations originating from research and development activities of the National Aeronautics and Space Administration. They emphasize information considered likely to be transferable across industrial, regional, or disciplinary lines and are issued to encourage commercial application.

Availability of NASA Tech Briefs and TSPs

Requests for individual Tech Briefs or for Technical Support Packages (TSPs) announced herein should be addressed to

National Technology Transfer Center

Telephone No. (800) 678-6882 or via World Wide Web at www2.nttc.edu/leads/

Please reference the control numbers appearing at the end of each Tech Brief. Information on NASA's Commercial Technology Team, its documents, and services is also available at the same facility or on the World Wide Web at www.nctn.hq.nasa.gov.

Commercial Technology Offices and Patent Counsels are located at NASA field centers to provide technology-transfer access to industrial users. Inquiries can be made by contacting NASA field centers and program offices listed below.

NASA Field Centers and Program Offices

Ames Research Center

Lisa L. Lockyer
(650) 604-3009
lisa.l.lockyer@nasa.gov

Dryden Flight Research Center

Gregory Poteat
(661) 276-3872
greg.poteat@dfrc.nasa.gov

Goddard Space Flight Center

Nona Cheeks
(301) 286-5810
Nona.K.Cheeks.1@gpsc.nasa.gov

Jet Propulsion Laboratory

Ken Wolfenbarger
(818) 354-3821
james.k.wolfenbarger@jpl.nasa.gov

Johnson Space Center

Charlene E. Gilbert
(281) 483-3809
commercialization@jsc.nasa.gov

Kennedy Space Center

Jim Aliberti
(321) 867-6224
Jim.Aliberti-1@ksc.nasa.gov

Langley Research Center

Jesse Midgett
(757) 864-3936
jesse.c.midgett@nasa.gov

John H. Glenn Research Center at Lewis Field

Larry Viterna
(216) 433-3484
cto@grc.nasa.gov

Marshall Space Flight Center

Vernotto McMillan
(256) 544-2615
vernotto.mcmillan@msfc.nasa.gov

Stennis Space Center

Robert Bruce
(228) 688-1929
robert.c.bruce@nasa.gov

NASA Program Offices

At NASA Headquarters there are seven major program offices that develop and oversee technology projects of potential interest to industry:

Carl Ray

Small Business Innovation Research Program (SBIR) & Small Business Technology Transfer Program (STTR)
(202) 358-4652 or
cray@nasa.gov

Benjamin Neumann

Innovative Technology Transfer Partnerships (Code TD)
(202) 358-2320
benjamin.j.neumann@nasa.gov

John Mankins

Office of Space Flight (Code TD)
(202) 358-4659 or
john.c.mankins@nasa.gov

Terry Hertz

Office of Aero-Space Technology (Code RS)
(202) 358-4636 or
thertz@nasa.gov

Glen Mucklow

Office of Space Sciences (Code SM)
(202) 358-2235 or
gmucklow@nasa.gov

Roger Crouch

Office of Microgravity Science Applications (Code U)
(202) 358-0689 or
rcrouch@nasa.gov

Granville Paules

Office of Mission to Planet Earth (Code Y)
(202) 358-0706 or
gpaules@mtpe.hq.nasa.gov



TECH BRIEFS

NATIONAL AERONAUTICS AND SPACE ADMINISTRATION



5 Technology Focus: Data Acquisition

- 5 Scheme for Entering Binary Data Into a Quantum Computer
- 5 Encryption for Remote Control via Internet or Intranet
- 6 Coupled Receiver/Decoders for Low-Rate Turbo Codes
- 7 Processing GPS Occultation Data To Characterize Atmosphere



9 Electronics/Computers

- 9 Displacing Unpredictable Nulls in Antenna Radiation Patterns
- 10 Integrated Pointing and Signal Detector for Optical Receiver
- 11 Adaptive Thresholding and Parameter Estimation for PPM



13 Software

- 13 Data-Driven Software Framework for Web-Based ISS Telescience
- 13 Software for Secondary-School Learning About Robotics
- 13 Fuzzy Logic Engine
- 13 Telephone-Directory Program
- 13 Simulating a Direction-Finder Search for an ELT



15 Materials

- 15 Formulating Precursors for Coating Metals and Ceramics
- 15 Making Macroscopic Assemblies of Aligned Carbon Nanotubes



17 Mechanics

- 17 Ball Bearings Equipped for *In Situ* Lubrication on Demand



19 Machinery/Automation

- 19 Synthetic Bursae for Robots
- 19 Robot Forearm and Dexterous Hand



21 Manufacturing

- 21 Making a Metal-Lined Composite-Overwrapped Pressure Vessel



23 Bio-Medical

- 23 *Ex Vivo* Growth of Bioengineered Ligaments and Other Tissues
- 24 Stroboscopic Goggles for Reduction of Motion Sickness
- 25 Articulating Support for Horizontal Resistive Exercise



27 Physical Sciences

- 27 Modified Penning-Malmberg Trap for Storing Antiprotons
- 28 Tumbleweed Rovers
- 28 Two-Photon Fluorescence Microscope for Microgravity Research



31 Information Sciences

- 31 Biased Randomized Algorithm for Fast Model-Based Diagnosis
- 31 Fast Algorithms for Model-Based Diagnosis



33 Books & Reports

- 33 Simulations of Evaporating Multicomponent Fuel Drops
- 33 Formation Flying of Tethered and Nontethered Spacecraft
- 33 Two Methods for Efficient Solution of the Hitting-Set Problem

This document was prepared under the sponsorship of the National Aeronautics and Space Administration. Neither the United States Government nor any person acting on behalf of the United States Government assumes any liability resulting from the use of the information contained in this document, or warrants that such use will be free from privately owned rights.



▶ Scheme for Entering Binary Data Into a Quantum Computer

This could be an important step toward making quantum computing practical.

NASA's Jet Propulsion Laboratory, Pasadena, California

A quantum algorithm provides for the encoding of an exponentially large number of classical data bits by use of a smaller (polynomially large) number of quantum bits (qubits). The development of this algorithm was prompted by the need, heretofore not satisfied, for a means of entering real-world binary data into a quantum computer. The data format provided by this algorithm is suitable for subsequent ultrafast quantum processing of the entered data. Potential applications lie in disciplines (e.g., genomics) in which one needs to search for matches between parts of very long sequences of data. For example, the algorithm could be used to encode the N -bit-long human genome in only $\log_2 N$ qubits. The resulting $\log_2 N$ -qubit state could then be used for subsequent quantum data processing — for example, to perform rapid comparisons of sequences.

Below are the steps of the algorithm, illustrated with the example of the four-bit string 0111:

1. Specify a correspondence between (a) each classical bit in a string of 2^n such bits and (b) a unique n -bit eigenstate in a set of 2^n such eigenstates. For example, if a classical 2^2 -bit string

is 0111, then the corresponding four 2-bit eigenstates could be $|00\rangle$, $|01\rangle$, $|10\rangle$, and $|11\rangle$.

2. Construct a superposition, $|\psi\rangle$, of equally weighted quantum states that is peaked at only those eigenstates that correspond to 1s in the classical bit string. In the example of the bit string 0111, the corresponding 2-qubit state would be $|\psi\rangle = 3^{-1/2}(|01\rangle+|10\rangle+|11\rangle)$. In the general case, the superposition would be an entangled state of n qubits that encodes a specific sequence of 2^n classical bits.
3. Compute the unitary transformation needed to obtain the superposition starting from an easy-to-make state (for example, $|00\rangle$). Equivalently, compute a unitary matrix that maps the chosen state (e.g., $|00\rangle$) into the state $|\psi\rangle$. For the classical bit string 0111, the unitary matrix would be

$$\begin{pmatrix} 0 & -1/\sqrt{3} & -1/\sqrt{3} & -1/\sqrt{3} \\ 1/\sqrt{3} & 2/3 & -1/3 & -1/3 \\ 1/\sqrt{3} & -1/3 & 2/3 & -1/3 \\ 1/\sqrt{3} & -1/3 & -1/3 & 2/3 \end{pmatrix}$$

To compute the matrix, first compute $|\psi\rangle\langle\psi|$ (which gives one column of the

matrix), then generate the remaining orthonormal vectors for the other columns.

4. By use of software developed previously for this purpose, compute the form of a feasible quantum circuit equivalent to the unitary matrix. The quantum circuit could be implemented in one of several physical embodiments: for example, spin-based, charge-based, optical, or superconducting quantum computer hardware.

This work was done by Colin Williams of Caltech for NASA's Jet Propulsion Laboratory. Further information is contained in a TSP (see page 1).

In accordance with Public Law 96-517, the contractor has elected to retain title to this invention. Inquiries concerning rights for its commercial use should be addressed to:

Innovative Technology Assets Management
JPL

Mail Stop 202-233
4800 Oak Grove Drive
Pasadena, CA 91109-8099
(818) 354-2240

E-mail: iaoffice@jpl.nasa.gov

Refer to NPO-30209, volume and number of this NASA Tech Briefs issue, and the page number.

▶ Encryption for Remote Control via Internet or Intranet

This protocol provides security against control by unauthorized users.

John F. Kennedy Space Center, Florida

A data-communication protocol has been devised to enable secure, reliable remote control of processes and equipment via a collision-based network, while using minimal bandwidth and computation. The network could be the Internet or an intranet. Control is made secure by use of both a password and a dynamic key, which is sent transparently to a remote user by the controlled computer (that is, the computer, located at the site of the equipment or process to be controlled,

that exerts direct control over the process). The protocol functions in the presence of network latency, overcomes errors caused by missed dynamic keys, and defeats attempts by unauthorized remote users to gain control. The protocol is not suitable for real-time control, but is well suited for applications in which control latencies up to about 0.5 second are acceptable.

The encryption scheme involves the use of both a dynamic and a private key, without any additional overhead

that would degrade performance. The dynamic key is embedded in the equipment- or process-monitor data packets sent out by the controlled computer: in other words, the dynamic key is a subset of the data in each such data packet. The controlled computer maintains a history of the last 3 to 5 data packets for use in decrypting incoming control commands. In addition, the controlled computer records a private key (password) that is given to the remote computer. The encrypted

incoming command is permuted by both the dynamic and private key. A person who records the command data in a given packet for hostile purposes cannot use that packet after the public key expires (typically within 3 seconds). Even a person in possession of an unauthorized copy of the command/remote-display software cannot use that software in the absence of the password.

The use of a dynamic key embedded in the outgoing data makes the central-processing unit overhead very small. The use of a National Instruments DataSocket™ (or equivalent) protocol or the User Datagram Protocol makes it possible to obtain reasonably short response times: Typical response times in event-driven control, using packets sized ≤ 300 bytes, are < 0.2 second for

commands issued from locations anywhere on Earth.

The protocol requires that control commands represent absolute values of controlled parameters (e.g., a specified temperature), as distinguished from changes in values of controlled parameters (e.g., a specified increment of temperature). Each command is issued three or more times to ensure delivery in crowded networks. The use of absolute-value commands prevents additional (redundant) commands from causing trouble. Because a remote controlling computer receives “talkback” in the form of data packets from the controlled computer, typically within a time interval ≤ 1 s, the controlling computer can re-issue a command if network failure has occurred.

The controlled computer, the process

or equipment that it controls, and any human operator(s) at the site of the controlled equipment or process should be equipped with safety measures to prevent damage to equipment or injury to humans. These features could be a combination of software, external hardware, and intervention by the human operator(s). The protocol is not fail-safe, but by adopting these safety measures as part of the protocol, one makes the protocol a robust means of controlling remote processes and equipment by use of typical office computers via intranets and/or the Internet.

This work was done by Lewis Lineberger of Kennedy Space Center. For further information, contact the Kennedy Commercial Technology Office at (321) 867-8130. KSC-12277

Coupled Receiver/Decoders for Low-Rate Turbo Codes

Residual carrier power needed for recovery of phase would be reduced.

NASA's Jet Propulsion Laboratory, Pasadena, California

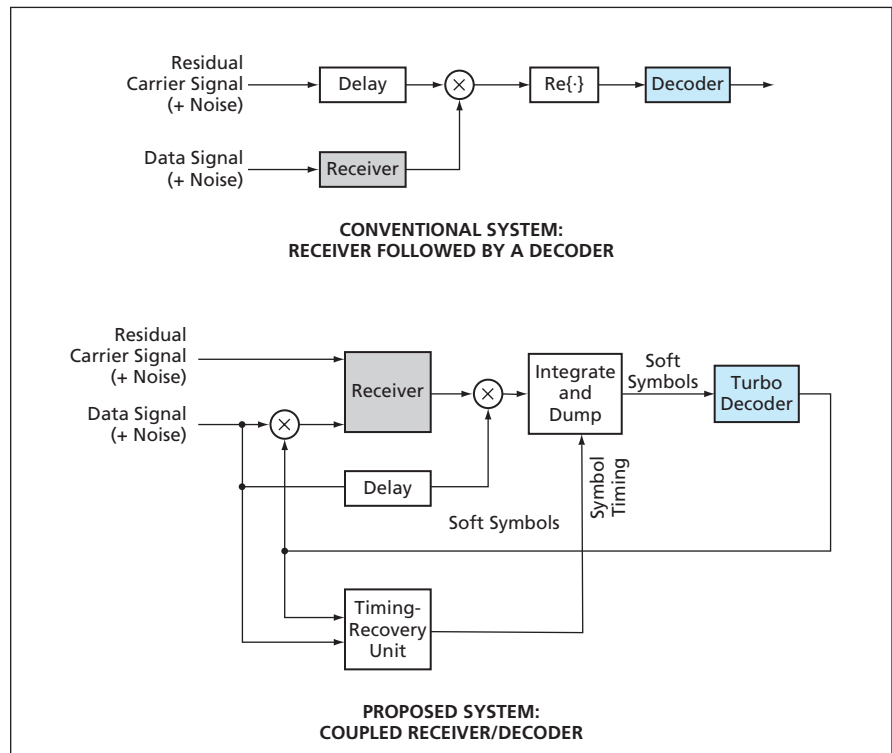
Coupled receiver/decoders have been proposed for receiving weak single-channel phase-modulated radio signals bearing low-rate-turbo-coded binary data. Originally intended for use in receiving telemetry signals from distant spacecraft, the proposed receiver/decoders may also provide enhanced reception in mobile radiotelephone systems.

A radio signal of the type to which the proposal applies comprises a residual carrier signal and a phase-modulated data signal. The residual carrier signal is needed as a phase reference for demodulation as a prerequisite to decoding. Low-rate turbo codes afford high coding gains and thereby enable the extraction of data from arriving radio signals that might otherwise be too weak. In the case of a conventional receiver, if the signal-to-noise ratio (specifically, the symbol energy to one-sided noise power spectral density) of the arriving signal is below approximately 0 dB, then there may not be enough energy per symbol to enable the receiver to recover properly the carrier phase. One could solve the problem at the transmitter by diverting some power from the data signal to the residual carrier. A better solution — a coupled receiver/decoder according to the proposal — could re-

duce the needed amount of residual carrier power.

In all that follows, it is to be understood that all processing would be digital and the incoming signals to be

processed would be, more precisely, outputs of analog-to-digital converters that preprocess the residual carrier and data signals at a rate of multiple samples per symbol. The upper part of the



A Coupled Receiver/Decoder would utilize data feedback from its turbo decoder, whereas a conventional receiver does not utilize data from the turbo decoder that follows it.

figure depicts a conventional receiving system, in which the receiver and decoder are uncoupled, and which is also called a non-data-aided system because output data from the decoder are not used in the receiver to aid in recovering the carrier phase. The receiver tracks the carrier phase from the residual carrier signal and uses the carrier phase to wipe phase noise off the data signal. The receiver typically includes a phase-locked loop (PLL) or Costas loop that requires no delay or perhaps a single sample delay.

The lower part of the figure depicts a basic coupled receiver/decoder — a data-aided system that would implement an iterative receiving/decoding process. The receiver would include a PLL or a Wiener filter that, to the extent possible, would track the residual carrier signal, wipe phase noise off the

data signal, then send the result to the turbo decoder. Recovery of timing could be effected by, for example, a digital transition tracking loop (DTTL) or other, similar loop. The first iteration of turbo decoding would yield soft data symbols, which would be sent back to the receiver for use in softly wiping off the data signal in an effort to recover the residual carrier signal. The wiped signal would contain a relatively large carrier-phase component that could be tracked by use of a second Wiener filter.

The refined phase estimate generated by the second Wiener filter would be used to wipe the phase noise from a delayed replica of the incoming data signal. The resulting refined data signal would then be sent to the turbo decoder for the second iteration. The soft symbols from the second iteration would be

sent back to the receiver as in the first iteration, and the process repeated.

For recovery of timing, the output of the turbo decoder would be used in place of what, in a usual DTTL, would be a transition-detector arm, in which hard decisions on consecutive symbols are based on raw symbol-by-symbol channel input, with no coding gain. The use of the turbo-decoder output would afford the benefit of the coding gain, thereby improving the output of the transition detector. Overall, the two-way communication between the receiver and the decoder would improve the performance of both the receiver and the decoder.

This work was done by Jon Hamkins and Dariush Divsalar of Caltech for NASA's Jet Propulsion Laboratory. Further information is contained in a TSP (see page 1). NPO-40237

Processing GPS Occultation Data To Characterize Atmosphere

NASA's Jet Propulsion Laboratory, Pasadena, California

GOAS [Global Positioning System (GPS) Occultation Analysis System] is a computer program that accepts signal-occultation data from GPS receivers aboard low-Earth-orbiting satellites and processes the data to characterize the terrestrial atmosphere and, in somewhat less comprehensive fashion, the ionosphere. GOAS is very robust and can be run in an unattended semi-operational processing mode. It features sophisticated retrieval algorithms that utilize the amplitudes and phases of the GPS signals. It incorporates a module that, using an assumed atmospheric

refractivity profile, simulates the effects of the retrieval processing system, including the GPS receiver. GOAS utilizes the GIPSY software for precise determination of orbits as needed for calibration. The GOAS output for the Earth's troposphere and mid-to-lower stratosphere consists of high-resolution (<1 km) profiles of density, temperature, pressure, atmospheric refractivity, bending angles of signals, and water-vapor content versus altitude from the Earth's surface to an altitude of 30 km. The GOAS output for the ionosphere consists of electron-density profiles

from an altitude of about 50 km to the altitude of a satellite, plus parameters related to the rapidly varying structure of the electron density, particularly in the E layer of the ionosphere.

This program was written by George Hajj, Emil Kursinski, Stephen Leroy, Byron Iijima, Manuel de la Torre Juarez, Larry Romans, and Chi Ao of Caltech for NASA's Jet Propulsion Laboratory. Further information is contained in a TSP (see page 1).

This software is available for commercial licensing. Please contact Don Hart of the California Institute of Technology at (818) 393-3425. Refer to NPO-30596.



Displacing Unpredictable Nulls in Antenna Radiation Patterns

A simple method could be implemented at minimal cost.

NASA's Jet Propulsion Laboratory, Pasadena, California

A method of maintaining radio communication despite the emergence of unpredictable fades and nulls in the radiation pattern of an antenna has been proposed. The method was originally intended to be applied in the design and operation of a radio antenna aboard a robotic exploratory vehicle on a remote planet during communication with a spacecraft in orbit around the planet. The method could also be applied in similar terrestrial situations — for example, radio communication between two ground vehicles or between a ground vehicle and an aircraft or spacecraft. The method is conceptually simple, is readily adaptable to diverse situations, and can be implemented without adding greatly to the weight, cost, power demand, or complexity of a system to which it may be applied.

The unpredictable fades and nulls in an antenna radiation pattern arise because of electromagnetic interactions between the antenna and other objects within the near field of the antenna (basically, objects within a distance of a few wavelengths). These objects can include general vehicle components, masts, robotic arms, other antennas, the ground, and nearby terrain features. Figure 1 presents representative plots of signal strength versus time during a typical pass of a spacecraft or aircraft through the far

field of such an antenna, showing typical nulls and fades caused by nearby objects.

The traditional approach to ensuring reliability of communication in the presence of deep fades calls for increasing the effective transmitter power and/or reducing the receiver noise figure at the affected ground vehicle, possibly in combination with appropriate redesign of the equipment at the spacecraft or aircraft end of the communication link. These solutions can be expensive and/or risky and, depending on the application, can add significantly to weight, cost, and power demand. The proposed method entails none of these disadvantages.

The essence of the proposed method is to shift the pattern of nulls and fades by switching electrical connections to parasitic radiating elements. The concept of parasitic radiating elements is not new by itself; parasitic radiators have been used to shape radiation patterns since the earlier years of antenna design. What is new here is the concept using parasitic radiators to shift patterns of nulls and fades, without regard for precise shaping of beams. In a typical operation, one or more parasitic radiator(s) would be switched when the distant communication terminal (spacecraft, aircraft, or ground vehicle) entered a deep fade or null. In the resulting shifted radiation pattern, the dis-

tant terminal would likely not be in a deep fade or null (see Figure 2), and so communication could continue.

A parasitic radiating element need not be of any particular design. For example, it could be a simple rigid or springy monopole antenna element approximately a quarter wavelength long. An electromechanical relay could be used to make or break an electrical connection between the base of the element and the chassis of the vehicle. Alternatively, a transistor switch could be used.

In many cases, it would not even be necessary to add components to act as parasitic radiating elements: some of the structures already present, including those that give rise to fades and nulls, could be used as switchable parasitic radiators. For example, an inductor having significant radio-frequency impedance but little DC resistance could be inserted in the grounding path of a robot in parallel with a short-circuiting switch. Then the radio-frequency properties of the arm would be changed and the pattern of nulls and fades shifted by switching between shorting or not shorting the inductor.

This work was done by James Lux and Mark Schaefer of Caltech for NASA's Jet Propulsion Laboratory. Further information is contained in a TSP (see page 1). NPO-30898

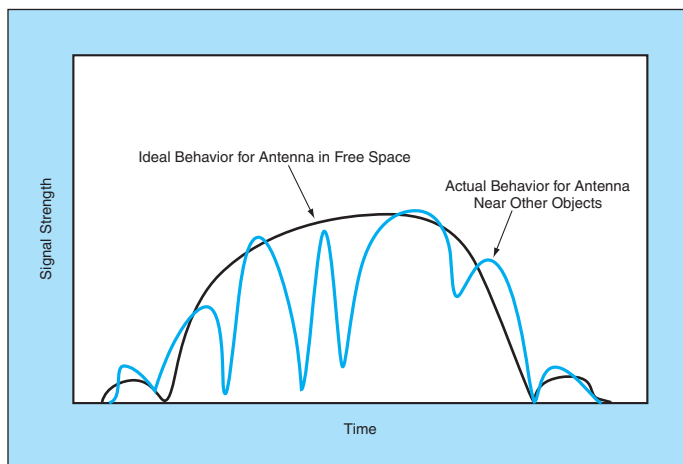


Figure 1. These Plots of Signal Strength Versus Time are typical of radio communication with a distant terminal crossing the beam of a stationary antenna. The relatively smooth plot would be obtained if the antenna were suspended in free space. In a more realistic case, nearby objects would give rise to deep fades.

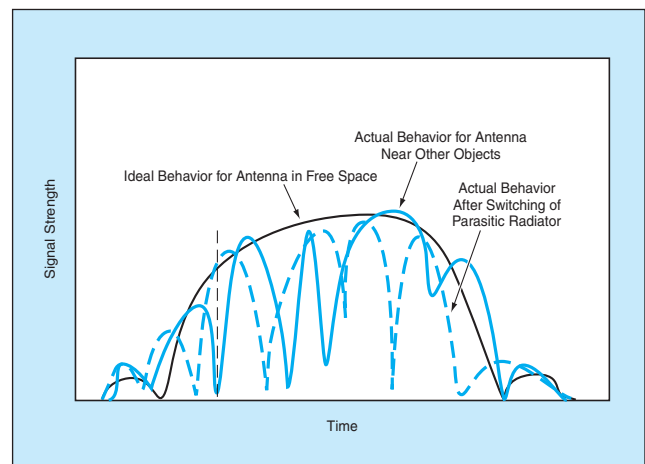


Figure 2. The Radiation Pattern Would Be Shifted and otherwise altered by switching of a parasitic radiator. At the time and position represented by the vertical dashed line, the distant terminal would be in a deep fade of the first radiation pattern but near a peak of the second (shifted) one.

Integrated Pointing and Signal Detector for Optical Receiver

Signal power would be utilized more efficiently and alignment would be less critical.

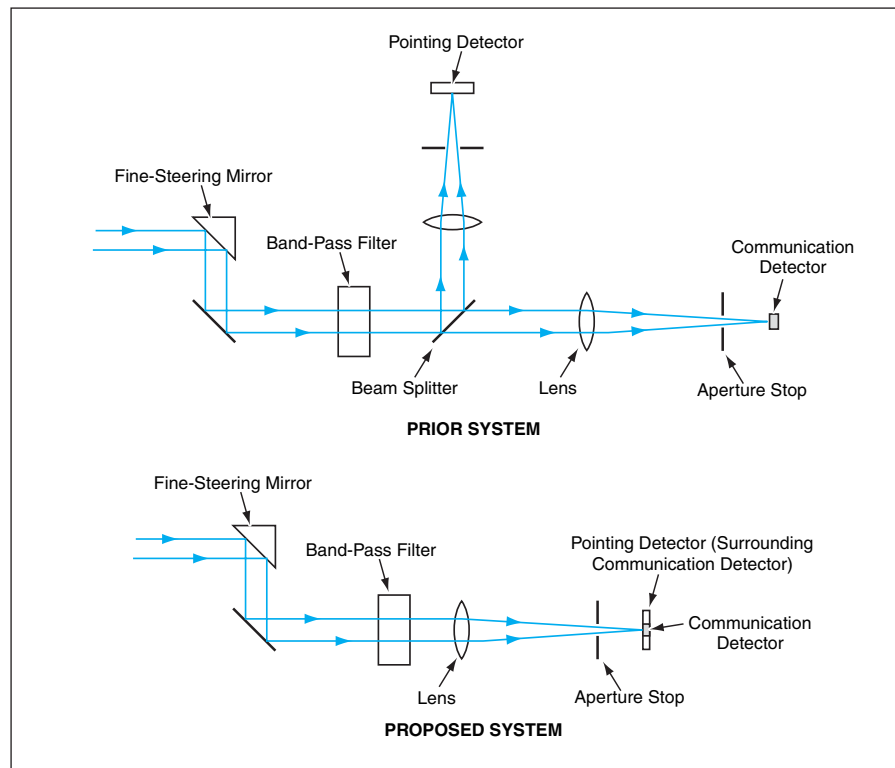
NASA's Jet Propulsion Laboratory, Pasadena, California

A design concept for the receiver portion of a proposed free-space optical-communication terminal calls for integration of its communication and pointing detectors. As explained below, this would entail a departure from prior designs, in which pointing and communication detectors have been separate.

As used here, "communication detector" denotes a single high-speed photodetector used for reception of a laser beam that has been modulated to convey information, while "pointing detector" denotes an array of photodetectors (typically, a quad-cell detector or a charge-coupled device) used in sensing the pointing error (the error in the aim of a receiver telescope, relative to the laser-beam axis). The pointing detector of this or any free-space optical-communication receiver is necessary for proper acquisition and tracking of the received laser beam. The suitably processed output of the pointing detector is fed back to a fine-steering mirror to reduce any pointing error and thereby maintain optimum reception.

Heretofore, it has been common practice to pass the incoming laser beam through a beam splitter that sends about 10 percent of the beam power to a pointing detector and the rest to a separate communication detector, as illustrated in the upper part of the figure. One disadvantage of this is that because only 10 percent of the received signal power is available for use by the pointing detector, the signal-to-noise ratio (SNR) at the pointing detector is lower than it otherwise would be. The performance of the pointing detector is correspondingly limited. Another disadvantage is that the alignment between the communication and pointing detectors is critical and must be ensured by means of a calibration procedure.

According to the proposal, there would be no beam splitter. The communication and pointing detectors would be positioned coaxially in the same focal plane, as shown in the lower part of the figure: the communication detector would occupy the central part of the focal plane, while the pointing detector would occupy the surrounding area. This arrangement would inherently ensure the proper alignment of the detectors with each other.



The **Pointing and Signal Detectors** are separate units on different output paths of a beam splitter in the prior system. In the proposed system, the pointing and signal detectors would be coaxial, integrated into a single unit.

The dimensions of the signal and pointing detectors would be chosen to take advantage of the Gaussian distribution of signal power in the focal plane. The communication detector would be sized to receive 85 percent of the received signal power at zero pointing error (in other words, when the received laser beam was centered on the focal plane). The reason for choosing this size is that it would maximize the SNR in the communication detector in the presence of background light.

During zero pointing error, the remaining 15 percent of the received signal power would impinge on the pointing detector. This would be half again as much signal power as is available to the pointing detector in the beam-splitter approach. Even more advantageously, during nonzero pointing error, the proportion of signal power available to the pointing detector would increase by a large amount because the Gaussian peak would no longer be centered on the communication detector. For example, if the pointing error were such as to

place the half-power radius of the beam at the center of the focal plane, then the power incident on the pointing detector would increase to five times that of the beam-splitter approach. This increase in power would help to make it possible to correct rapidly for large pointing disturbances — for example, those caused by wind.

This work was done by Michael Britcliffe and Daniel Hoppe of Caltech for NASA's Jet Propulsion Laboratory. Further information is contained in a TSP (see page 1).

In accordance with Public Law 96-517, the contractor has elected to retain title to this invention. Inquiries concerning rights for its commercial use should be addressed to:

*Innovative Technology Assets Management
JPL*

*Mail Stop 202-233
4800 Oak Grove Drive
Pasadena, CA 91109-8099
(818) 354-2240*

E-mail: iaoffice@jpl.nasa.gov

Refer to NPO-30647, volume and number of this NASA Tech Briefs issue, and the page number.

Adaptive Thresholding and Parameter Estimation for PPM

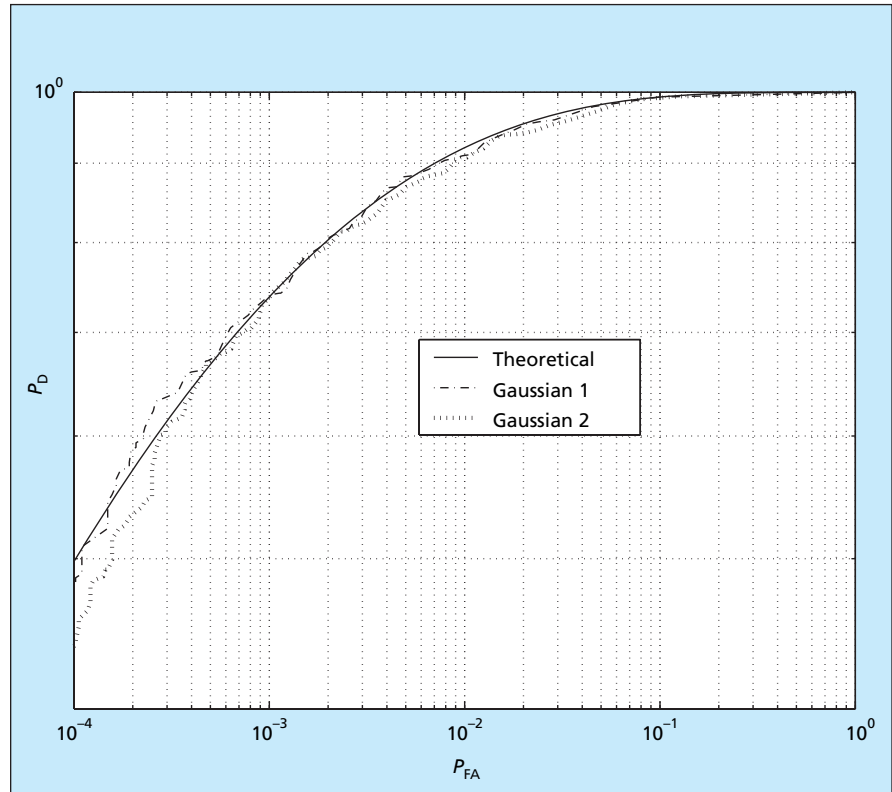
A receiver detection threshold is repeatedly adjusted to balance competing requirements.

NASA's Jet Propulsion Laboratory, Pasadena, California

A method of adaptive setting of a threshold level for the detection of pulses in a pulse-position modulation (PPM) free-space optical communication system has been developed. In simplified terms, it is desirable to set a threshold value high enough to greatly reduce the probability (P_{FA} as defined below) of erroneously detecting noise as signal pulses but not so high as to greatly reduce the probability (P_D as defined below) of detecting any signal pulses that may be present along with noise. In the present method, the threshold level is varied with time, in response to changing conditions in the optical-communication channel, in an effort to maintain a balance between the aforesaid competing requirements. An integral part of this adaptation scheme is a scheme for estimating key parameters of the optical-communication channel in particular, parameters that describe the fading and total attenuation in the channel, and parameters that characterize spreading of pulses by atmospheric and other effects. The method can be implemented by software processing of digitized optoelectronic-detector output, and has been tested by computational simulation.

In the first stage of processing by this method, the digitized values of the detector output during noise-only time slots of received PPM symbols are averaged to obtain a background level. This background level is subtracted from the detector output in the hope of reducing or eliminating the noise component in the remaining signal. (This background level should not be confused with the detection threshold, which is computed in the last stage of processing.) Next, the remaining signal — in effect, a vector of pulse samples — is normalized by dividing it by its L_1 norm (in general, the L_1 norm of a vector is defined as the sum of absolute magnitudes of its orthogonal components).

In the next stage of processing, the vector is analyzed to obtain the pulse-spreading parameters: The vector is presented to a radial-basis-function neural network that has been trained to recognize the shape of the normalized pulses as either (1) an abrupt rise followed by an exponential decay of



This ROC Curve for was calculated theoretically for $\beta = 0.29$ for an ideal pulse shape and by computational simulation for two different Gaussian-spread pulse shapes. The detection threshold of the receiver is chosen to place the receiver operating point at a desired location on this curve.

characteristic time τ or (2) a Gaussian peak characterized by a spreading time σ . An additional advantage of normalization is that it increases reliability by reducing the likelihood that the network would be confused by differences in pulse amplitudes caused by fading. The output of the network consists of (1) an indication of whether the pulses are deemed to be exponential or Gaussian in shape and (2) the numerical value of τ or σ , whichever is applicable.

The reliability of the averaged PPM symbols presented to the network can be increased by using a (255, 223) Reed-Solomon code to detect and remove defective PPM symbols and shot-noise events that are erroneously detected as PPM symbols. The average is computed anew for each code word. The total of 255 received symbols in each code word are decoded to 223 information symbols, which are, in turn, re-encoded to 255 “corrected” symbols. The “corrected” symbols are compared

with the original 255 received symbols. Only those original symbols that agree with the corresponding re-encoded symbols are used in computing the average.

The fade parameter, α , is a linear function of the L_1 norm. There exists a family of such linear functions that have different slopes corresponding to different values of the pulse-spread parameters τ and σ . Given the applicable value of τ or σ , the appropriate curve is selected, then its slope computed and used in conjunction with the calculated value of the L_1 norm to estimate α . The attenuation parameter, β , equals the product of α and an analytic function. The choice of analytic function depends on whether the pulses have been determined to be Gaussian or exponential; in either case, the independent variable is the ratio between the duration (T_s) of a pulse time slot and the applicable pulse-spread parameter.

A receiver operating characteristic (ROC) curve is used in the next stage of

processing. The ROC curve (see figure) is equivalent to a plot of the probability of detection (P_D) versus the false-alarm probability (P_{FA}). More precisely, P_D is the probability of successful detection of a PPM pulse when such a pulse is present; P_{FA} is the probability that the detector output noise will exceed the signal-

detection threshold and thereby cause the detection of a PPM pulse when such a pulse is not present. It turns out that the ROC curve depends primarily on β , and the location of the receiver operating point on the ROC depends primarily on the detection threshold, λ . The final step is to choose the value of λ that

strikes the required balance between P_D and P_{FA} .

*This work was done by Payman Arabshahi, Ryan Mulai, and Tsun-Yee Yan of Caltech for NASA's Jet Propulsion Laboratory. Further information is contained in a TSP (see page 1).
NPO-40714*

2 Data-Driven Software Framework for Web-Based ISS Telescience

Software that enables authorized users to monitor and control scientific payloads aboard the International Space Station (ISS) from diverse terrestrial locations equipped with Internet connections is undergoing development. This software reflects a data-driven approach to distributed operations. A Web-based software framework leverages prior developments in Java and Extensible Markup Language (XML) to create portable code and portable data, to which one can gain access via Web-browser software on almost any common computer. Open-source software is used extensively to minimize cost; the framework also accommodates enterprise-class server software to satisfy needs for high performance and security. To accommodate the diversity of ISS experiments and users, the framework emphasizes openness and extensibility. Users can take advantage of available viewer software to create their own client programs according to their particular preferences, and can upload these programs for custom processing of data, generation of views, and planning of experiments. The same software system, possibly augmented with a subset of data and additional software tools, could be used for public outreach by enabling public users to replay telescience experiments, conduct their experiments with simulated payloads, and create their own client programs and other custom software.

This program was written by Kam S. Tso of IA Tech, Inc. for Marshall Space Flight Center. Further information is contained in a TSP (see page 1). MFS-31848

⚙ Software for Secondary-School Learning About Robotics

The ROVER Ranch is an interactive computer program designed to help secondary-school students learn about space-program robotics and related basic scientific concepts by involving the students in simplified design and programming tasks that exercise skills in mathematics and science. The tasks

involve building simulated robots and then observing how they behave. The program furnishes (1) programming tools that a student can use to assemble and program a simulated robot and (2) a virtual three-dimensional mission simulator for testing the robot. First, the ROVER Ranch presents fundamental information about robotics, mission goals, and facts about the mission environment. On the basis of this information, and using the aforementioned tools, the student assembles a robot by selecting parts from such subsystems as propulsion, navigation, and scientific tools, the student builds a simulated robot to accomplish its mission. Once the robot is built, it is programmed and then placed in a three-dimensional simulated environment. Success or failure in the simulation depends on the planning and design of the robot. Data and results of the mission are available in a summary log once the mission is concluded.

This program was written by Robert O. Shelton of Johnson Space Center, Stephanie L. Smith of LinCom, and Dat Truong and Terry R. Hodgson of Science Applications International Corp. For further information, contact the Johnson Commercial Technology Office at (281) 483-3809. MSC-23595

2 Fuzzy Logic Engine

The Fuzzy Logic Engine is a software package that enables users to embed fuzzy-logic modules into their application programs. Fuzzy logic is useful as a means of formulating human expert knowledge and translating it into software to solve problems. Fuzzy logic provides flexibility for modeling relationships between input and output information and is distinguished by its robustness with respect to noise and variations in system parameters. In addition, linguistic fuzzy sets and conditional statements allow systems to make decisions based on imprecise and incomplete information. The user of the Fuzzy Logic Engine need not be an expert in fuzzy logic: it suffices to have a basic understanding of how linguistic rules can be applied to the user's problem. The Fuzzy Logic Engine is divided into two modules: (1) a graphical-interface software tool for creating linguistic fuzzy sets and conditional statements and (2) a

fuzzy-logic software library for embedding fuzzy processing capability into current application programs. The graphical-interface tool was developed using the Tcl/Tk programming language. The fuzzy-logic software library was written in the C programming language.

This program was written by Ayanna Howard of Caltech for NASA's Jet Propulsion Laboratory. Further information is contained in a TSP (see page 1).

This software is available for commercial licensing. Please contact Don Hart of the California Institute of Technology at (818) 393-3425. Refer to NPO-40461.

2 Telephone-Directory Program

eDirectory is a computer program that makes it possible to view entries in the Jet Propulsion Laboratory (JPL) telephone directory by use of PalmPilot™ (or equivalent) personal digital assistants. When one uses eDirectory, a single click causes the downloading of a current copy of the directory (which is updated nightly) from a server. The downloaded directory data can be sorted and searched. The program can append a "JPL" category and save directory information in a file that can be imported into the Palm Desktop™ software.

This program was written by William Vlahos of Caltech for NASA's Jet Propulsion Laboratory. Further information is contained in a TSP (see page 1).

This software is available for commercial licensing. Please contact Don Hart of the California Institute of Technology at (818) 393-3425. Refer to NPO-30427.

⚙ Simulating a Direction-Finder Search for an ELT

A computer program simulates the operation of direction-finding equipment engaged in a search for an emergency locator transmitter (ELT) aboard an aircraft that has crashed. The simulated equipment is patterned after the equipment used by the Civil Air Patrol to search for missing aircraft. The program is designed to be used for training in radio direction-finding and/or searching for missing aircraft without incurring the expense and risk of using real aircraft and ground search resources. The program places a hidden ELT on a map and enables the user to search for the location of the ELT by moving a

small aircraft image around the map while observing signal-strength and direction readings on a simulated direction-finding locator instrument. As the simulated aircraft is turned and moved on the map, the program updates the readings on the direction-finding instrument to reflect the current position and

heading of the aircraft relative to the location of the ELT. The software is distributed in a zip file that contains an installation program. The software runs on the Microsoft Windows 9x, NT, and XP operating systems.

*This program was written by Bruce Bream of **Glenn Research Center**. Fur-*

ther information is contained in a TSP (see page 1).

Inquiries concerning rights for the commercial use of this invention should be addressed to NASA Glenn Research Center, Commercial Technology Office, Attn: Steve Fedor, Mail Stop 4-8, 21000 Brookpark Road, Cleveland Ohio 44135. Refer to LEW 17485-1.



Formulating Precursors for Coating Metals and Ceramics

John H. Glenn Research Center, Cleveland, Ohio

A protocol has been devised for formulating low-vapor-pressure precursors for protective and conversion coatings on metallic and ceramic substrates. The ingredients of a precursor to which the protocol applies include additives with phosphate esters, or aryl phosphate esters in solution. Additives can include iron, chromium, and/or other transition metals. Alternative or additional additives can include magnesium compounds to facilitate growth of films on substrates that do not contain magnesium.

Formulation of a precursor begins with mixing of the ingredients into a

high-vapor-pressure solvent to form a homogeneous solution. Then the solvent is extracted from the solution by evaporation — aided, if necessary, by vacuum and/or slight heating. The solvent is deemed to be completely extracted when the viscosity of the remaining solution closely resembles the viscosity of the phosphate ester or aryl phosphate ester. In addition, satisfactory removal of the solvent can be verified by means of a differential scanning calorimetry essay: the absence of endothermic processes for temperatures below 150 °C would indicate that

the residual solvent has been eliminated from the solution beyond a detectable dilution level.

This work was done by Wilfredo Morales of Glenn Research Center and Jorge E. Gatica and John T. Reye of Cleveland State University. Further information is contained in a TSP (see page 1).

Inquiries concerning rights for the commercial use of this invention should be addressed to NASA Glenn Research Center, Commercial Technology Office, Attn: Steve Fedor, Mail Stop 4-8, 21000 Brookpark Road, Cleveland, Ohio 44135. Refer to LEW-17537-1.

Making Macroscopic Assemblies of Aligned Carbon Nanotubes

Nanotubes are aligned and manipulated with the help of magnetic and/or electric fields.

Lyndon B. Johnson Space Center, Houston, Texas

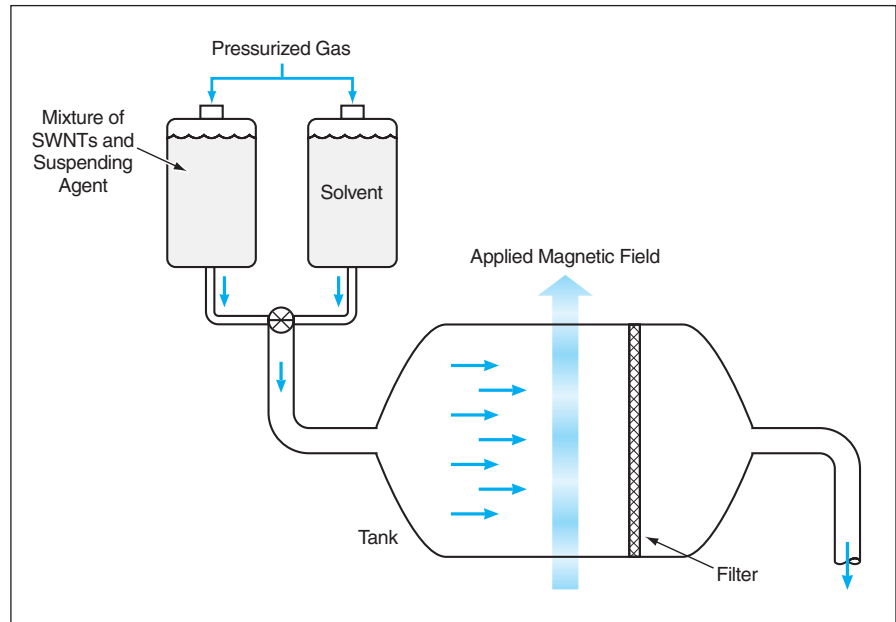
A method of aligning and assembling single-wall carbon nanotubes (SWNTs) to fabricate macroscopic structures has been invented. The method entails suspending SWNTs in a fluid, orienting the SWNTs by use of a magnetic and/or electric field, and then removing the aligned SWNTs from suspension in such a way as to assemble them while maintaining the alignment.

SWNTs are essentially tubular extensions of fullerene molecules. It is desirable to assemble aligned SWNTs into macroscopic structures because the common alignment of the SWNTs in such a structure makes it possible to exploit, on a macroscopic scale, the unique mechanical, chemical, and electrical properties that individual oriented SWNTs exhibit at the molecular level. Because of their small size and high electrical conductivity, carbon nanotubes, and especially SWNTs, are useful for making electrical connectors in integrated circuits. Carbon nanotubes can be used as antennas at optical frequencies, and as probes in scanning tunneling microscopes, atomic-force microscopes, and the like. Carbon nanotubes can be used with or instead of carbon black in tires. Carbon nanotubes are

useful as supports for catalysts. Ropes of SWNTs are metallic and, as such, are potentially useful in some applications in which electrical conductors are needed — for example, they could be used as additives in formulating electrically con-

ductive paints. Finally, macroscopic assemblies of aligned SWNTs can serve as templates for the growth of more and larger structures of the same type.

The great variety of tubular fullerene molecules and of the structures that



A Solution Containing Suspended SWNTs is made to flow through a magnetic field and a filter. The magnetic field orients the SWNTs predominantly parallel with each other in the plane of the filter. Hence, the SWNTs become deposited on the filter in alignment with each other.

could be formed by assembling them in various ways precludes a complete description of the present method within the limits of this article. It must suffice to present a typical example of the use of one of many possible variants of the method to form a membrane comprising SWNTs aligned substantially parallel to each other in the membrane plane. The apparatus used in this variant of the method (see figure) includes a reservoir containing SWNTs dispersed in a suspending agent (for example, dimethylformamide) and a reservoir containing a suitable solvent (for example, water mixed with a surfactant). By use of either pressurized gas supplied from upstream or suction from downstream, the suspension of SWNTs and the solvent are forced to mix and flow into a tank. A filter inside the tank contains pores small enough to prevent the passage of most SWNTs, but large enough to allow the passage of molecules of the solvent and suspending agent. The filter is oriented perpendicular to the flow path. A magnetic field parallel to the plane of the filter is applied.

The success of the method is based on the tendency of SWNTs to become

aligned with their longitudinal axes parallel to an applied magnetic field. The alignment energy of an SWNT increases with the length of the SWNT and the magnetic-field strength. In order to obtain an acceptably small degree of statistical deviation of SWNTs of a given length from alignment with a magnetic field, one must make the field strong enough so that the thermal energy associated with rotation of an SWNT away from alignment is less than the alignment energy.

As the liquid passes through the filter, the aligned (more precisely, partially aligned) SWNTs become trapped on the filter. As SWNTs accumulate on the filter, they become attached to each other by van der Waals forces, thereby assembling themselves into a membrane. The flow of liquid and suspended SWNTs can be continued until the membrane has grown to the desired thickness, which would typically be of the order of 1 μm or more.

The membrane is removed from the screen, then subjected to a rinsing and drying process that removes the suspending agent and allows the SWNTs to come into more intimate contact, in-

creasing the degree of van der Waals contact and thereby effectively strengthening bonds between adjacent aligned SWNTs. Further alignment and increase in the degree of van der Waals contact is achieved by annealing the membrane in an inert atmosphere at a temperature between 200 and 1,300 $^{\circ}\text{C}$. Membranes consisting mostly of aligned SWNTs, with thicknesses $>1 \mu\text{m}$ and areas $>1 \text{cm}^2$, have been produced by this method.

This work was done by Richard E. Smalley, Daniel T. Colbert, Ken A. Smith, Deron A. Walters, Michael J. Casavant, Xiaochuan Qin, Boris Yakobson, Robert H. Hauge, Rajesh Kumar Saini, Wan-Ting Chiung, and Charles B. Huffman of Rice University for Johnson Space Center.

In accordance with Public Law 96-517, the contractor has elected to retain title to this invention. Inquiries concerning rights for its commercial use should be addressed to:

*William Marsh Rice University
Office of Technology Transfer MS-705
P.O. Box 1892
Houston, TX 77251-1892*

Refer to MSC-23302, volume and number of this NASA Tech Briefs issue, and the page number.

⊕ Ball Bearings Equipped for *In Situ* Lubrication on Demand

Operational lifetimes can be prolonged.

John H. Glenn Research Center, Cleveland, Ohio

In situ systems that provide fresh lubricants to ball/race contacts on demand have been developed to prolong the operational lives of ball bearings. These systems were originally intended to be incorporated into ball bearings in mechanisms that are required to operate in outer space for years, in conditions in which lubricants tend to deteriorate and/or evaporate. These systems may also be useful for similarly prolonging bearing lifetimes on Earth.

Reservoirs have been among the means used previously to resupply lubricants. Lubricant-resupply reservoirs are bulky and add complexity to bearing assemblies. In addition, such a reservoir cannot be turned on or off as needed: it supplies lubricant continuously, often leading to an excess of lubricant in the bearing.

A lubricator of the present type includes a porous ring cartridge attached to the inner or the outer ring of a ball bearing (see Figure 1). Oil is stored in the porous cartridge and is released by heating the cartridge: Because the thermal expansion of the oil exceeds that of the cartridge, heating causes the ejection of some oil. A metal film can be deposited on a face of the cartridge to serve as an electrical-resistance heater. The heater can be activated in response to a measured increase in torque that signals depletion of oil from the bearing/race contacts.

Because the oil has low surface tension and readily wets the bearing-ring material, it spreads over the bearing ring and eventually reaches the ball/race contacts. The Marangoni effect (a surface-tension gradient associated with a temperature gradient) is utilized to enhance the desired transfer of lubricant to the ball/race contacts during heating.

For a test, a ball bearing designed for use at low speed was assembled without lubricant and equipped with a porous-ring lubricator, the resistance heater of which consumed a power of less than 1 W when triggered on by a torque-measuring device. In the test, a load of 20 lb (≈ 89 N) was applied and the bearing was turned at a rate of 200 RPM. The lubricator control was turned on at the beginning of the test, turned off for about 800 seconds, then

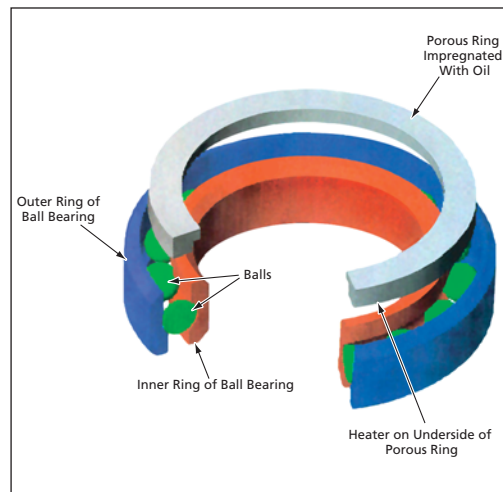


Figure 1. A **Porous Ring** impregnated with oil is attached to one of the ball-bearing rings. When the porous ring is heated, some oil is squeezed out. The oil then spreads over the bearing surface and eventually reaches the bearing/race contacts.

turned on again. As shown in Figure 2, the controlled lubricator stabilized the torque in a low range, starting immediately after initial turn-on and immediately after resumption of the lubricator control.

This work was done by Mario Marchetti of National Research Council; William R. Jones, Jr., and Stephen V. Pepper of Glenn Research Center; Mark Jansen of Sest, Inc.; and Roamer Predmore of Goddard Space Flight Center. Further information is contained in a TSP (see page 1).

Inquiries concerning rights for the commercial use of this invention should be addressed to NASA Glenn Research Center, Commercial Technology Office, Attn: Steve Fedor, Mail Stop 4-8, 21000 Brookpark Road, Cleveland Ohio 44135. Refer to LEW-17414.

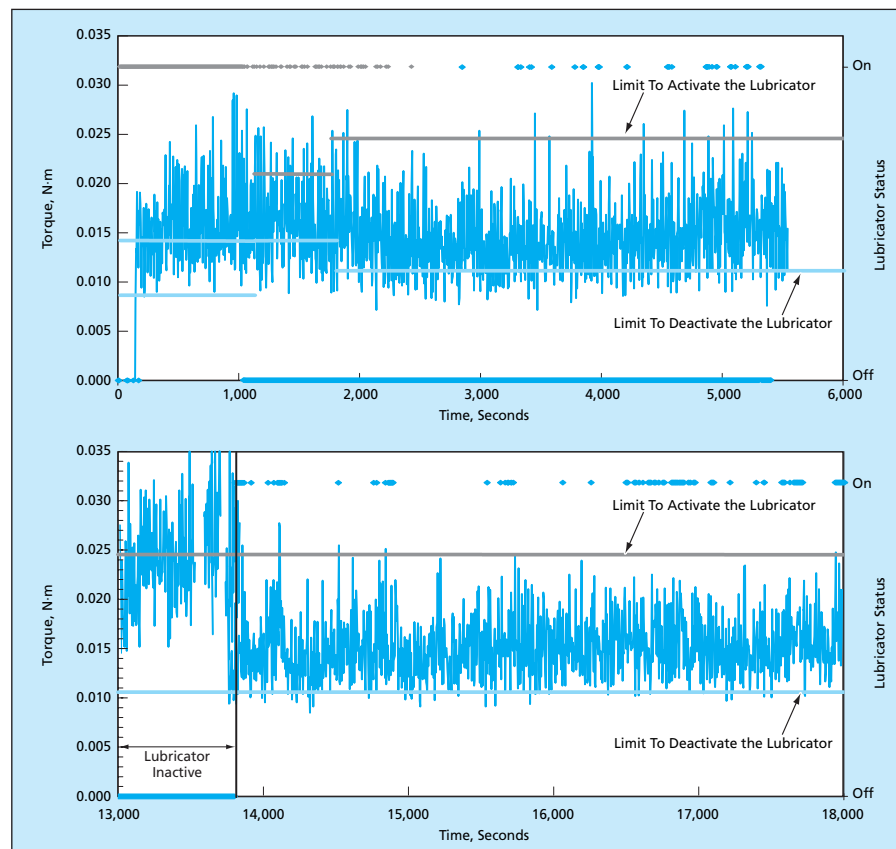


Figure 2. **Ball-Bearing Torque** was maintained within a low range by using a lubricator as described in the text to dispense lubricant as needed.

⚙️ Synthetic Bursae for Robots

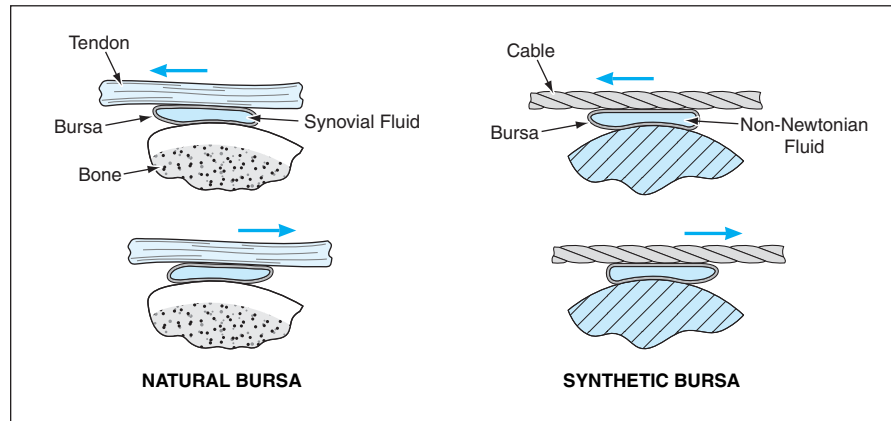
Functions would be similar to those of natural bursae.

Lyndon B. Johnson Space Center, Houston, Texas

Synthetic bursae are under development for incorporation into robot joints that are actuated by motor-driven cables in a manner similar to that of arthropod joints actuated by muscle-driven tendons. Like natural bursae, the synthetic bursae would serve as cushions and friction reducers.

A natural bursa is a thin bladder filled with synovial fluid, which serves to reduce friction and provide a cushion between a bone and a muscle or a tendon (see figure). A synthetic bursa would be similar in form and function: It would be, essentially, a compact, soft roller consisting of a bladder filled with a non-Newtonian fluid. The bladder would be constrained to approximately constant volume. The synthetic bursa would cushion an actuator cable against one of the members of a robot joint and would reduce the friction between the cable and the member. Under load, the pressure in the bladder would hold the opposite walls of the bladder apart, making it possible for them to move freely past each other without rubbing.

A synthetic bursa could be made by fabricating a bladder from a composite of lock-woven mesh and strong elas-



A Bursa, whether natural or synthetic, is a bladder that contains a cushioning, friction-reducing fluid; it functions essentially as a soft roller.

tomer and filling the bladder with a non-Newtonian fluid. Depending on the specific application, it could be advantageous to use a dilatant or a thixotropic fluid. Ideally, a synthetic bursa would be designed so that it would bottom out before reaching its burst pressure. In the bottomed-out condition, the opposite walls would slide past each other on an almost capillary film of the non-Newtonian fluid.

At the time of reporting the information for this article, prototype synthetic bursae with simple spherical shapes were being fabricated. Subsequent prototypes would have more complex shapes somewhat like those of natural bursae.

This work was done by Christopher S. Louchik of Johnson Space Center. For further information, contact the Johnson Commercial Technology Office at (281) 483-3809. MSC-23064.

⚙️ Robot Forearm and Dexterous Hand

The hand is highly anthropomorphic and even includes a folding palm.

Lyndon B. Johnson Space Center, Houston, Texas

An electromechanical hand-and-forearm assembly has been developed for incorporation into an anthropomorphic robot that would be used in outer space. The assembly is designed to offer manual dexterity comparable to that of a hand inside an astronaut's suit; thus, the assembly may also be useful as a prosthesis or as an end effector on an industrial robot.

The assembly has a total of 14 degrees of freedom. It consists of a forearm, which houses the motors and drive electronics; a two-degree-of-freedom wrist; and a five-finger, 12-degree-of-freedom hand. The hand itself is broken down into two sections: a dexterous

work set, which is used for manipulation, and a grasping set, which allows the hand to maintain a stable grasp while manipulating or actuating a given object. The dexterous set consists of two three-degree-of-freedom fingers (pointer and index) and a three-degree-of-freedom opposable thumb. The grasping set consists of two, one-degree-of-freedom fingers (ring and pinkie) and a palm.

The fingers are powered by motors mounted in the forearm (see figure). Mechanical power for the fingers is transmitted through the wrist via flex shafts. In the hand, small modular lead-

screw assemblies convert the rotary motion of the flex shafts to linear motion. The outer shells of the leadscrew assemblies are instrumented as load cells to provide force feedback.

The leadscrews are linked to the fingers by short cables that lie in cammed grooves in the fingers. The use of cables reduces (in comparison with the use of gears or other drive mechanisms) the size and complexity of the fingers while allowing the fingers to be very compliant in the non-driven direction. The cammed grooves keep the bend radii of the cables large to prevent excessive stressing of the cables.

Two leadscrew assemblies that work in a differential manner drive the two-degree-of-freedom base joint of the dexterous fingers. The two distal pitch

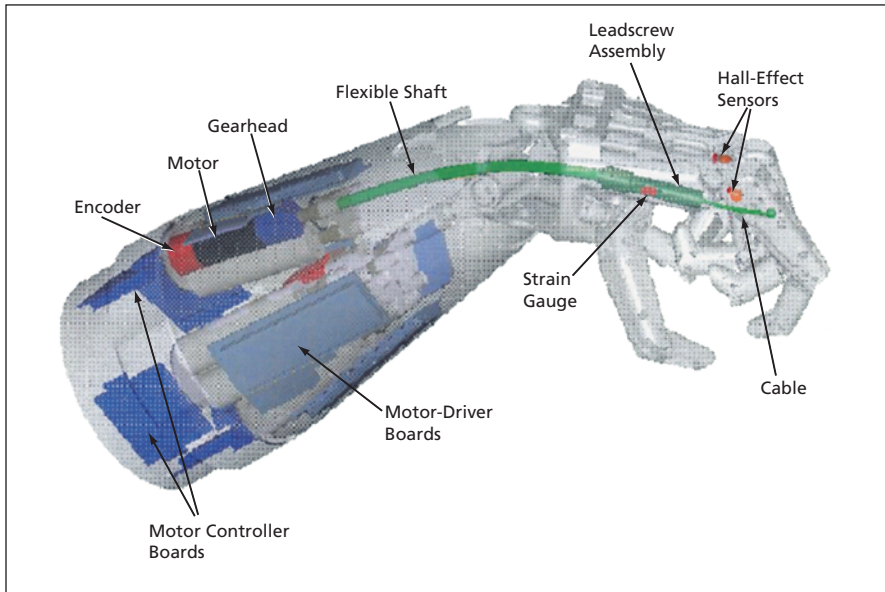
joints of these fingers are linked and driven by a third leadscrew assembly through a decoupling link in the base of the finger. The thumb is driven in a

manner similar to that of the dexterous fingers, except that the base joints are skewed and the yaw is exaggerated in order to match the motion of the human thumb. In the gripping fingers, all three degrees of freedom are linked and are driven by one leadscrew assembly. Both of the gripping fingers are mounted on pivoting bases and driven by another leadscrew assembly in order to enable the palm to cup inward, allowing the hand to conform to an object being held.

The wrist is designed as a large open hook joint (to allow the flexible shafts to pass through) and is driven by two linear actuators. The forearm is 4 in. (≈ 10 cm) in diameter at the base and 8 in. (≈ 20 cm) long.

This work was done by Christopher S. Lovchik of Johnson Space Center.

This invention is owned by NASA, and a patent application has been filed. Inquiries concerning nonexclusive or exclusive license for its commercial development should be addressed to the Patent Counsel, Johnson Space Center, (281) 483-0837. Refer to MSC-22883.



One of the Finger Drive Trains is emphasized in this view of the robot forearm and hand. The motive forces for the fingers are generated in the forearm and are transmitted to the fingers by flexible shafts, leadscrews, and cables.

Making a Metal-Lined Composite-Overwrapped Pressure Vessel

The metal liner reduces loss of gas by diffusion without adding much weight.

Marshall Space Flight Center, Alabama

A process has been devised for the fabrication of a pressure vessel that comprises a composite-material (matrix/fiber) shell with a metal liner on its inner surface. The use of the composite material makes it possible for the tank to be strong enough to withstand the anticipated operating pressure and yet weigh less than does an equivalent all-metal tank. The metal liner is used

as a barrier against permeation: In the absence of such a barrier, the pressurized gas in the tank could leak by diffusing through the composite-material shell.

The figure depicts workpieces at four key stages in the process, which consists of the following steps:

1. A mandrel that defines the size and shape of the pressure vessel is made

by either molding or machining a piece of tooling wax.

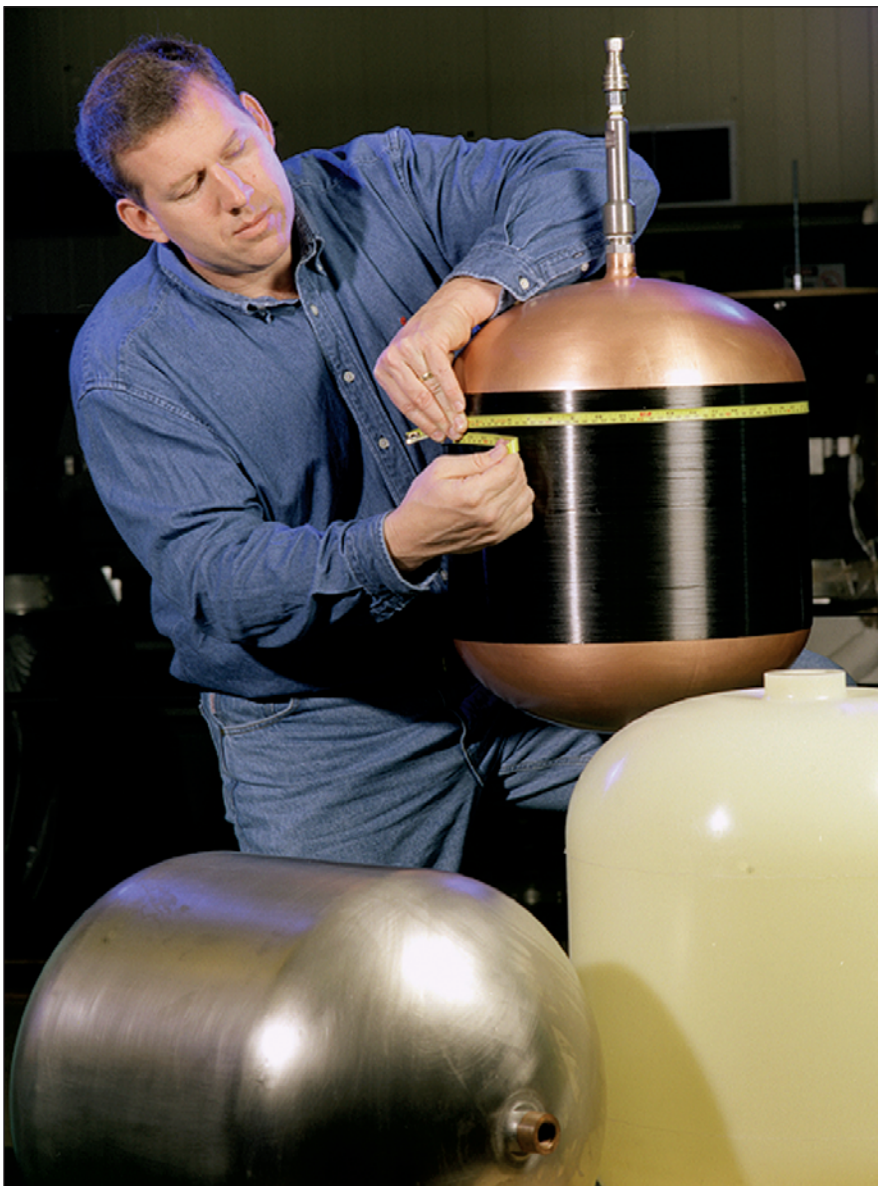
2. Silver paint is applied to the surface of the mandrel to make it electrically conductive.
3. The ends of the mandrel are fitted with metal bosses.
4. The mandrel is put into a plating bath, wherein the metal liner is electrodeposited. Depending on the applications, the liner metal could be copper, nickel, gold, or an alloy. Typical liner thicknesses range from 1 to 10 mils (0.025 to 0.25 mm).
5. The wax is melted from within, leaving the thin metal liner.
6. A hollow shaft that includes holes and fittings through which the liner can be pressurized is sealed to both ends of the liner. The liner is pressurized to stiffen (and hence stabilize) it for the next step.
7. The pressurized liner is placed in a filament-winding machine, which is then operated to cover the liner with multiple layers of an uncured graphite-fiber/epoxy-matrix or other suitable composite material.
8. The composite-overwrapped liner is cured in an oven.
9. The pressure is relieved and the shaft is removed. The tank is then ready for use.

The process as described above accommodates variations:

- The mandrel could be made of a wax that melts at a higher temperature and not removed until the tank is cured in the oven.
- The tank need not be cylindrical or axisymmetric, as long as the filament-winding machine can accommodate the chosen shape.
- Shallow grooves could be formed on the surface of the mandrel to give the liner a bellowslike character for reinforcement and/or to accommodate expansion and contraction.

This work was done by Tom DeLay of Marshall Space Flight Center.

This invention is owned by NASA, and a patent application has been filed. For further information, contact Sammy Nabors, MSFC Commercialization Assistance Lead, at sammy.a.nabors@nasa.gov. Refer to MFS-31814.



A Wax Mandrel (on the bottom right) defines the size and shape of a composite-overwrapped metal liner (top center) that, after further processing, becomes a lightweight pressure vessel. Sample on the bottom left shows a mandrel coated with silver paint before it is placed into a plating bath.



Ex Vivo Growth of Bioengineered Ligaments and Other Tissues

Lifelike mechanical loads cause cell cultures to grow into lifelike structures.

Lyndon B. Johnson Space Center, Houston, Texas

A method of growing bioengineered tissues for use in surgical replacement of damaged anterior cruciate ligaments has been invented. An anterior cruciate ligament is one of two ligaments (the other being the posterior cruciate ligament) that cross in the middle of a knee joint and act to prevent the bones in the knee from sliding forward and backward relative to each other. Anterior cruciate liga-

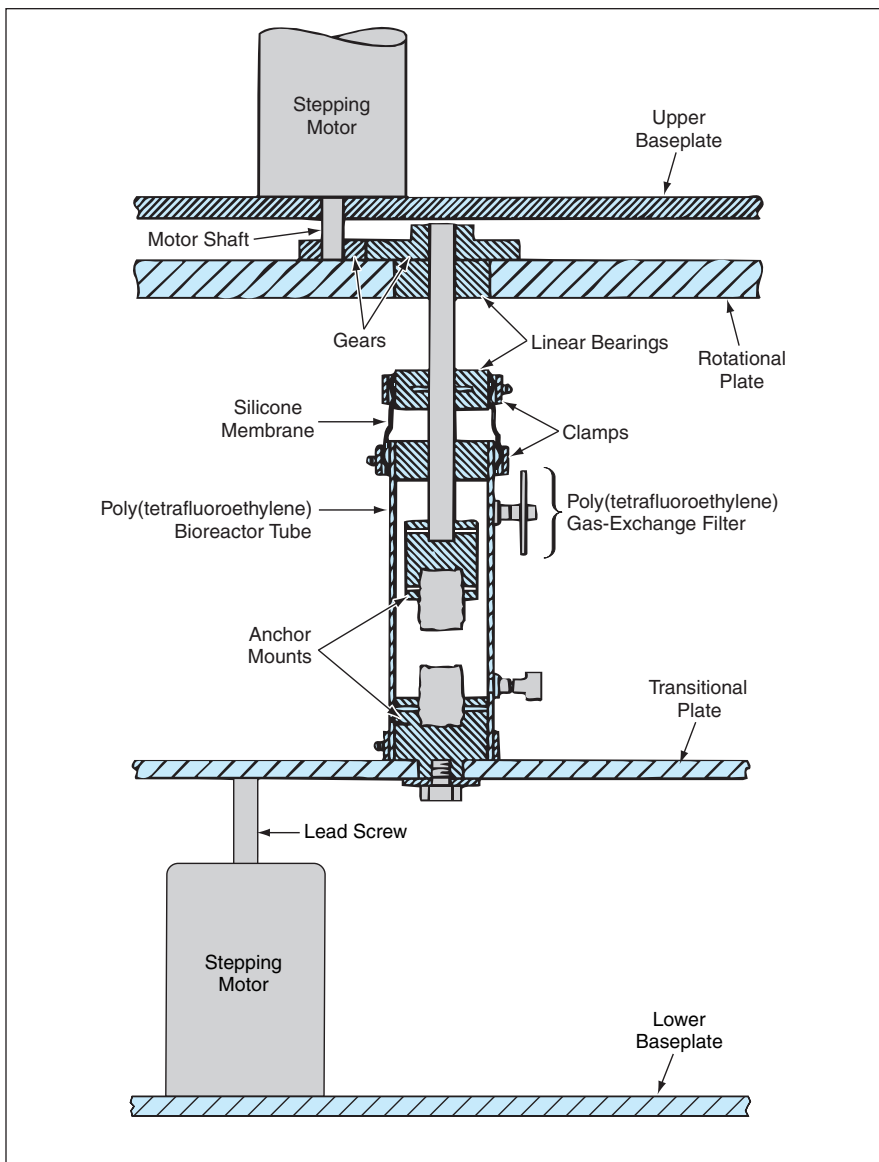
ments are frequently torn in sports injuries and traffic accidents, resulting in pain and severe limitations on mobility. By making it possible to grow replacement anterior cruciate ligaments that structurally and functionally resemble natural ones more closely than do totally synthetic replacements, the method could create new opportunities for full or nearly full restoration of functionality

in injured knees. The method is also adaptable to the growth of bioengineered replacements for other ligaments (e.g., other knee ligaments as well as those in the hands, wrists, and elbows) and to the production of tissues other than ligaments, including cartilage, bones, muscles, and blood vessels.

The method is based on the finding that the histomorphological properties of a bioengineered tissue grown *in vitro* from pluripotent cells within a matrix are affected by the direct application of mechanical force to the matrix during growth generation. This finding provides important new insights into the relationships among mechanical stress, biochemical and cell-immobilization methods, and cell differentiation, and is applicable to the production of the variety of tissues mentioned above. Moreover, this finding can be generalized to nonmechanical (e.g., chemical and electromagnetic) stimuli that are experienced *in vivo* by tissues of interest and, hence, the method can be modified to incorporate such stimuli in the *ex vivo* growth of replacements for the various tissues mentioned above.

In this method, a three-dimensional matrix made of a suitable material is seeded with pluripotent stem cells. The patient's bone-marrow stromal cells are preferably used as the pluripotent cells in this method. Suitable matrix materials are materials to which cells can adhere — for example, collagen type I. The seeded matrix is attached to anchors at opposite ends and then the cells in the matrix are cultured under conditions appropriate for the growth and regeneration of cells. Suitable anchor materials are materials to which the matrix can attach; examples include demineralized bone and Goinopra coral that has been treated to convert its calcium carbonate to calcium phosphate.

During the growth process, the matrix is subjected to a combination of tension, compression, torsion, and shear stresses via movement of one or both of the anchors. The figure depicts the combination of (1) a bioreactor tube within which the growth process takes place



The **Anchor Mounts Inside the Bioreactor Tube** are rotated and translated by two stepping-motor-driven mechanisms during growth of a cell culture in a matrix attached to the anchor mounts. The motions impose stresses like those experienced by the cells *in vivo*.

and (2) an apparatus that operates under computer control to generate the required motions. Optimally, the stresses should mimic those to which the anterior cruciate ligament is subjected *in vivo* during normal activity. The bioengineered ligament produced by this method is characterized by a cellular orientation and/or matrix crimp pattern in the direction of the applied mechanical forces, and by the production of collagen type I, collagen type III, and fi-

bronectin proteins along the axis of mechanical loading. Optimally, the ligament thus produced contains fiber bundles arranged in a helical pattern.

This work was done by Gregory Altman, David L. Kaplan, Ivan Martin, and Gordana Vunjak-Novakovic of Massachusetts Institute of Technology for Johnson Space Center.

In accordance with Public Law 96-517, the contractor has elected to retain title to this invention. Inquiries concerning rights for its

commercial use should be addressed to:

*Technology Licensing Office
Massachusetts Institute of Technology
Five Cambridge Center, Kendall Square
Room NE25-230
Cambridge, MA 02142-1493
Phone: (617) 253-6966
Fax: (617) 258-6790
E-mail: tlo@mit.edu*

Refer to MSC-23351, volume and number of this NASA Tech Briefs issue, and the page number.

Stroboscopic Goggles for Reduction of Motion Sickness

The view is presented to wearer in snapshots to suppress retinal slip.

Lyndon B. Johnson Space Center, Houston, Texas

A device built around a pair of electronic shutters has been demonstrated to be effective as a prototype of stroboscopic goggles or eyeglasses for preventing or reducing motion sickness. The momentary opening of the shutters helps to suppress a phenomenon that is known in the art as retinal slip and is described more fully below.

While a number of different environmental factors can induce motion sickness, a common factor associated with every known motion environment is sensory confusion or sensory mismatch. Motion sickness is a product of misinformation arriving at a central point in the nervous system from the senses from which one determines one's spatial orientation. When information from the eyes, ears, joints, and pressure receptors are all in agreement as to one's orientation, there is no motion sickness. When one or more sensory input(s) to the

brain is not expected, or conflicts with what is anticipated, the end product is motion sickness.

Normally, an observer's eye moves, compensating for the anticipated effect of motion, in such a manner that the image of an object moving relatively to an observer is held stationary on the retina. In almost every known environment that induces motion sickness, a change in the gain (in the signal-processing sense of "gain") of the vestibular system causes the motion of the eye to fail to hold images stationary on the retina, and the resulting motion of the images is termed retinal slip.

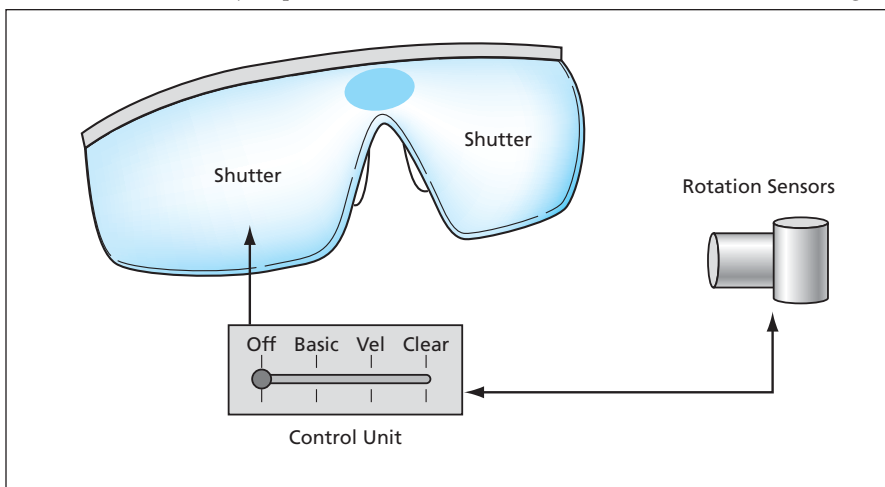
The present concept of stroboscopic goggles or eyeglasses (see figure) is based on the proposition that prevention of retinal slip, and hence, the prevention of sensory mismatch, can be expected to reduce the tendency toward motion sickness. A device according to

this concept helps to prevent retinal slip by providing snapshots of the visual environment through electronic shutters that are brief enough that each snapshot freezes the image on each retina. The exposure time for each snapshot is less than 5 ms. In the event that a higher rate of strobing is necessary for adequate viewing of the changing scene during rapid head movements, the rate of strobing (but not the exposure time) can be controlled in response to the readings of rate-of-rotation sensors attached to the device.

The shutters are compact, fast-acting, low-voltage, low-current liquid-crystal display devices of the polymer-dispersed liquid-crystal type. The shutters are installed in the lens spaces in the goggle or eyeglass frame. Sensors that measure the rates of rotation about the yaw and pitch axis are attached to the frame. Also included is a controller unit that contains a low-frequency oscillator and a switchable driver that receives the rotation-sensor readings. As now envisioned, a user of a production version of the device could select any of at least four basic modes of operation:

- Mode 1: The device would be turned off.
- Mode 2: The shutters would be held transparent, allowing ordinary vision.
- Mode 3: The shutters would open at a standard stroboscopic flash rate of 4 Hz.
- Mode 4: The flash rate would be adjusted according to the sensed rates of rotation. The maximum flash rate would be 40 Hz.

The standard flash rate of 4 Hz was chosen partly on the basis of effectiveness in suppressing motion sickness and



A Pair of Goggles or Eyeglasses contains electronic shutters in place of or in addition to lenses. The shutters can be strobed at either a constant rate or a rate that depends on the rates of yaw and pitch of the wearer's head.

partly because it is low enough not to trigger seizures in most individuals afflicted with photosensitive epilepsy. (Approximately one person in 10,000 has photosensitive epilepsy, which is triggered by a number of visual phenomena, including, in most cases, lights flashing

at rates between 15 and 20 Hz.) Preferably, individuals who have any form of epilepsy or any of a number of related disorders should not use this device.

This work was done by M. F. Reschke of Johnson Space Center and Jeffrey T. Somers of Wyle Laboratories.

This invention is owned by NASA, and a patent application has been filed. Inquiries concerning nonexclusive or exclusive license for its commercial development should be addressed to the Patent Counsel, Johnson Space Center, (281) 483-0837. Refer to MSC-23444.

Articulating Support for Horizontal Resistive Exercise

Supports can be optimized for a variety of prescribed exercises.

Lyndon B. Johnson Space Center, Houston, Texas

A versatile mechanical device provides support for a user engaged in any of a variety of resistive exercises in a substantially horizontal orientation. The unique features and versatility of the device promise to be useful in bed-rest studies, rehabilitation, and specialized strength training. The device affords a capability for selectively loading and unloading of portions of the user's body through its support mechanisms, so that specific parts of the body can be trained with little or no effect on other parts that may be disabled or in the process of recovery from injury. Thus, the device is ideal for rehabilitation exercise programs prescribed by physicians and physical therapists. The capability for selective loading and support also offers potential benefits to strength and conditioning trainers and athletes who wish to selectively strengthen selected parts.

The principal innovative aspect of the device is that it supports the subject's weight while enabling the subject, lying substantially horizontally, to perform an exercise that closely approximates a full

standing squat. The device includes mechanisms that support the subject in such a way that the hips are free to translate both horizontally and vertically and are free to rotate about the line connecting the hips. At the same time, the shoulders are free to translate horizontally while the upper back is free to rotate about the line connecting the shoulders.

Among the mechanisms for hip motion and support is a counterbalance that offsets the weight of the subject as the subject's pelvis translates horizontally and vertically and rotates the pelvis about the line connecting the hips. The counterbalance is connected to a pelvic support system that allows these pelvic movements. The subject is also supported at the shoulder by a mechanism that can tilt to provide continuous support of the upper back while allowing the rotation required for arching the back as the pelvis is displaced. The shoulder support also affords a capability for horizontal motion, and acts as the point of attachment of a load that is provided for squat and heel-raise exercises. The

device is compatible with any resistive-exercise machine that provides bilateral loading via a moving cable or other mechanical linkage.

The hip-translation and shoulder-translation and -rotation degrees of freedom of the supports can be locked individually or in combination in order to support the subject as necessary for exercises other than the standing squat. If necessary, for such exercises, the load can be applied directly to the subject by use of various attachments. In addition to the aforementioned heel raise, such exercises include the upright row, leg press, curls, extension of the triceps, front raise, lateral raise, and rear raise.

This work was done by Daniel Gundo of Ames Research Center and Grant Schaffner, Jason Bentley, and James A. Loehr of Wyle Laboratories for Johnson Space Center.

This invention is owned by NASA, and a patent application has been filed. Inquiries concerning nonexclusive or exclusive license for its commercial development should be addressed to the Patent Counsel, Johnson Space Center, (281) 483-0837. Refer to MSC-23594.



Modified Penning-Malmberg Trap for Storing Antiprotons

One set of electrodes is used for both transmission and reception.

Marshall Space Flight Center, Alabama

A modified Penning-Malmberg trap that could store a small cloud of antiprotons for a relatively long time (weeks) has been developed. This trap is intended for use in research on the feasibility of contemplated future matter/antimatter-annihilation systems as propulsion sources for

spacecraft on long missions. This trap is also of interest in its own right as a means of storing and manipulating antiprotons for terrestrial scientific experimentation.

The use of Penning-Malmberg traps to store antiprotons is not new. What is new here is the modified trap design, which utilizes state-of-the-art radio-frequency (RF) techniques, including ones that, heretofore, have been used in radio-communication applications but not in ion-trap applications.

A basic Penning-Malmberg trap includes an evacuated round tube that contains or is surrounded by three or more collinear tube electrodes. A steady axial magnetic field that reaches a maximum at

the geometric center of the tube is applied by an external source, and DC bias voltages that give rise to an electrostatic potential that reaches a minimum at the center are applied to the electrodes. The combination of electric and magnetic fields confines the charged particles (ions or electrons) for which it was designed to a prolate spheroidal central region. However, geometric misalignments and the diffusive cooling process prevent the steady fields of a basic Penning-Malmberg trap from confining the particles indefinitely.

In the modified Penning-Malmberg trap, the loss of antiprotons is reduced or eliminated by use of a "rotating-wall" RF stabilization scheme that also heats the antiproton cloud to minimize loss by matter/antimatter annihilation. The scheme involves the superposition of a quadrupole electric field that rotates about the cylindrical axis at a suitably chosen radio frequency.

The modified Penning-Malmberg trap (see Figure 1) includes several collinear sets of electrodes inside a tubular vacuum chamber. Each set comprises either a single metal tube or else a tube that is segmented into four electrodes that subtend equal angles about the cylindrical axis. The output of an RF signal generator is fed through a 90° hybrid coupler and then through two baluns to generate four replicas of the signal at relative phase shifts of 0°, 90°, 180°, and 270° (see Figure 2). These signal replicas are fed through -6-dB directional couplers, then via coaxial cables to the vacuum chamber. The signal is then routed to a phase cancellation network, which filters out the drive signal with the difference representing the plasma interaction. Inside the vacuum chamber, twisted-pair wires feed the signals from the coaxial cables to the four electrodes of each segmented electrode tube.

It is not necessary to use a different set of electrodes for moni-

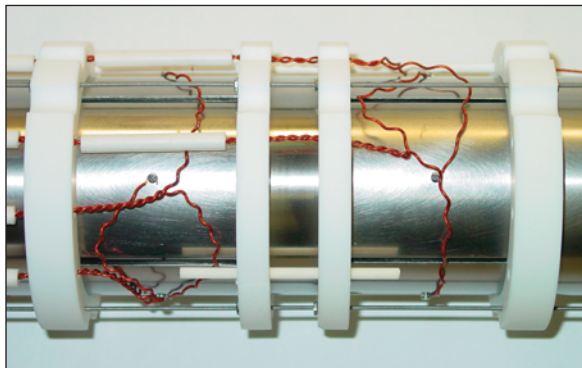


Figure 1. The **Modified Penning-Malmberg Trap** includes electrode tubes separated by insulating rings. Some of the tubes are segmented into four electrodes each.

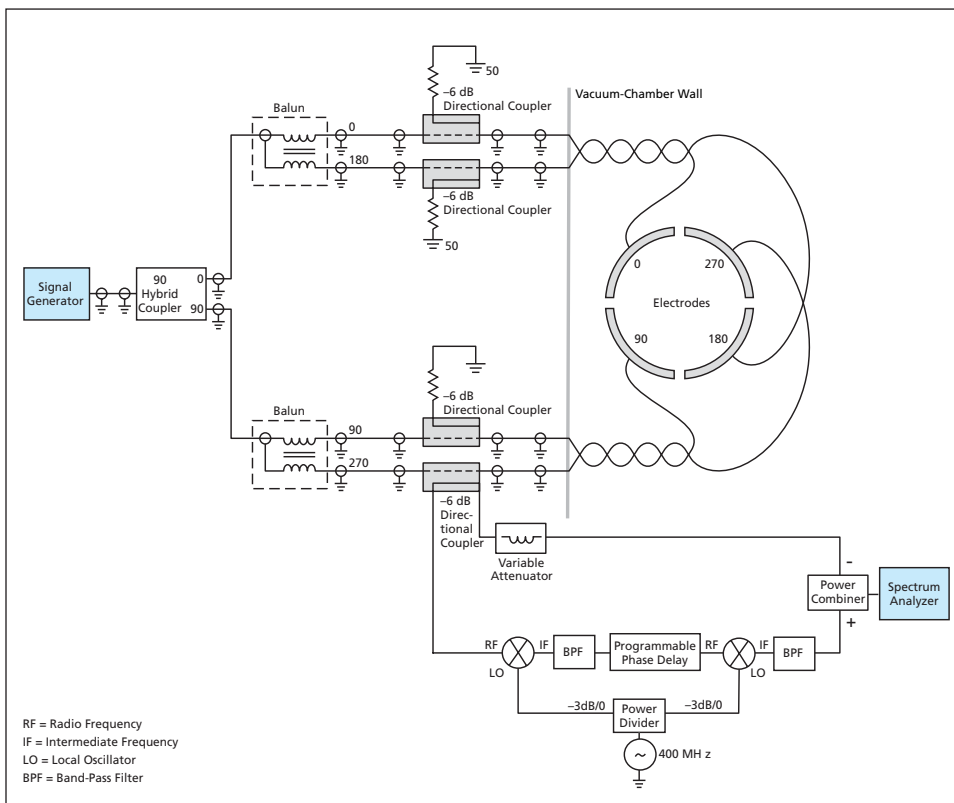


Figure 2. This **Radio-Frequency Circuit** enables simultaneous application of the RF stabilizing signal and monitoring of the RF response of the cloud of antiprotons confined in the trap.

toring the antiproton cloud. Instead, the -6-dB directional couplers are used to receive the signal that emanates from the antiproton cloud when the cloud interacts with the applied signal. The received signal can be routed to either a spectrum analyzer or a network analyzer.

This work was done by William H. Sims and James Martin of Marshall Space Flight Center, and Raymond Lewis of RLewis Co. Further information is contained in a TSP (see page 1).

This invention is owned by NASA, and a patent application has been filed. Inquiries

concerning nonexclusive or exclusive license for its commercial development should be addressed to the Patent Counsel, Marshall Space Flight Center, (256) 544-0021. Refer to MFS-31780.

Tumbleweed Rovers

Lightweight balls containing scientific instruments are propelled across terrain by wind.

NASA's Jet Propulsion Laboratory, Pasadena, California

Tumbleweed rovers, now undergoing development, are lightweight, inflatable, approximately spherical exploratory robotic vehicles designed to roll across terrain, using only wind for propulsion. Tumbleweed rovers share many features with "beach-ball" rovers, which were discussed in several prior *NASA Tech Briefs* articles. Conceived for use in exploring remote planets, tumbleweed rovers could also be used for exploring relatively inaccessible terrain on Earth.

A fully developed tumbleweed rover would consist of an instrumentation package suspended in an inflated two-layer (nylon/polypropylene) ball. The total mass of the rover would be of the order of 10 kg, the diameter of the ball when inflated would be 2 meters, and the minimum wind speed needed for propulsion would be about 5 m/s. The instrumentation package would contain

a battery power supply, sensors, a Global Positioning System (GPS) receiver, and a radio transmitter that would send the sensor readings and the GPS position and time readings to a monitoring station via a satellite communication system. Depending on the specific exploratory mission, the sensors could include a thermometer, a barometer, a magnetometer (for studying the terrestrial magnetic field and/or detecting buried meteorites), a subsurface radar system (for measuring ice thickness and/or detecting buried meteorites), and/or one or two diametrically opposed cameras that would take the part of sending two side-looking images out.

In the planned Antarctic field test, a prototype tumbleweed rover was released at a location near the South Pole. Using the global Iridium satellite network to send information about its position, the

rover transmitted temperature, pressure, humidity, and light intensity data to NASA's Jet Propulsion Laboratory. The rover reached speeds of 30 km per hour over the Antarctic ice cap, and traveled at an average speed of about 6 km per hour. The test was designed to confirm the rover's long-term durability in an extremely cold environment, with the goal being eventual use of the device to explore the Martian polar caps and other planets in the solar system. On future Antarctic exploratory missions, tumbleweed rovers might be used to acquire sensor data for studies of global warming, ozone depletion, and impacts of meteorites.

*This work was done by Alberto Behar, Jack Jones, Frank Carsey, and Jaret Matthews of Caltech for NASA's Jet Propulsion Laboratory. Further information is contained in a TSP (see page 1).
NPO-40499*

Two-Photon Fluorescence Microscope for Microgravity Research

The benefits of two-photon fluorescence microscopy are realized at reduced cost.

John H. Glenn Research Center, Cleveland, Ohio

A two-photon fluorescence microscope has been developed for the study of biophysical phenomena. Two-photon microscopy is a novel form of laser-based scanning microscopy that enables three-dimensional imaging without many of the problems inherent in confocal microscopy. Unlike one-photon optical microscopy, two-photon microscopy utilizes the simultaneous nonlinear absorption of two near-infrared photons. However, the efficiency of two-photon absorption is much lower than that of one-photon absorption, so an ultra-fast pulsed laser source is typically employed.

On the other hand, the critical energy threshold for two-photon absorption leads

to fluorophore excitation that is intrinsically localized to the focal volume. Consequently, two-photon microscopy enables optical sectioning and confocal performance without the need for a signal-limiting pinhole. In addition, there is a reduction (relative to one-photon optical microscopy) in photon-induced damage because of the longer excitation wavelength. This reduction is especially advantageous for *in vivo* studies. Relative to confocal microscopy, there is also a reduction in background fluorescence, and, because of a reduction in Rayleigh scattering, there is a 4 \times increase of penetration depth.

The prohibitive cost of a commercial two-photon fluorescence-microscope sys-

tem, as well as a need for modularity, has led to the construction of a custom-built system (see Figure 1). This system includes a coherent mode-locked titanium:sapphire laser emitting 120-fs-duration pulses at a repetition rate of 80 MHz. The pulsed laser has an average output power of 800 mW and a wavelength tuning range of 700 to 980 nm, enabling the excitation of a variety of targeted fluorophores. The output from the laser is attenuated, spatially filtered, and then directed into a confocal scanning head that has been modified to provide for side entry of the laser beam. The laser output coupler has been replaced with a dichroic filter that reflects the longer-wavelength excitation

light and passes the shorter-wavelength fluorescence light. Also, the confocal pin-hole has been removed to increase the signal strength.

The laser beam is scanned by a two-perpendicular-axis pair of galvanometer mirrors through a pupil transfer lens into the side port of an inverted microscope. Finally, the beam is focused by a 63-magnification, 1.3-numerical-aperture oil-immersion objective lens onto a specimen. The pupil transfer lens serves to match the intermediate image planes of the scanning head and the microscope, and its location is critical.

In order to maximize the quality of the image, (that is, the point spread function of the objective lens for all scan positions), the entire system was modeled in optical-design software, and the various free design parameters (the parameters of the spatial-filter components as well as the separations of all of the system components) were determined through an iterative optimization process. A modular design was chosen to facilitate access to the optical train for future fluorescence correlation spectroscopy and fluorescence-lifetime experiments.

The spatial resolution of the microscope at an excitation wavelength of 780 nm was measured by scanning a 170-nm-diameter fluorescent bead throughout the focal region and found to be 320 nm in the transverse direction and 740 nm in the longitudinal direction. The sectioning capability of two-photon microscopy is demonstrated in Figure 2, which depicts a human bone specimen as imaged by use of two-channel spectral detection.

The two-photon microscope is now being employed to study osteoblast and osteoclast bone cells in cultures, including the effects of fluid flow and other environmental stimuli. Ultimately, these studies will be used to investigate and develop effective countermeasures to the bone loss experienced in a reduced-gravity environment. In addition, a variant of this instrument is being considered as an add-on module to the Light Microscopy Module, which will be deployed on the International Space Station.

This work was done by David G. Fischer and Gregory A. Zimmerli of Glenn Research

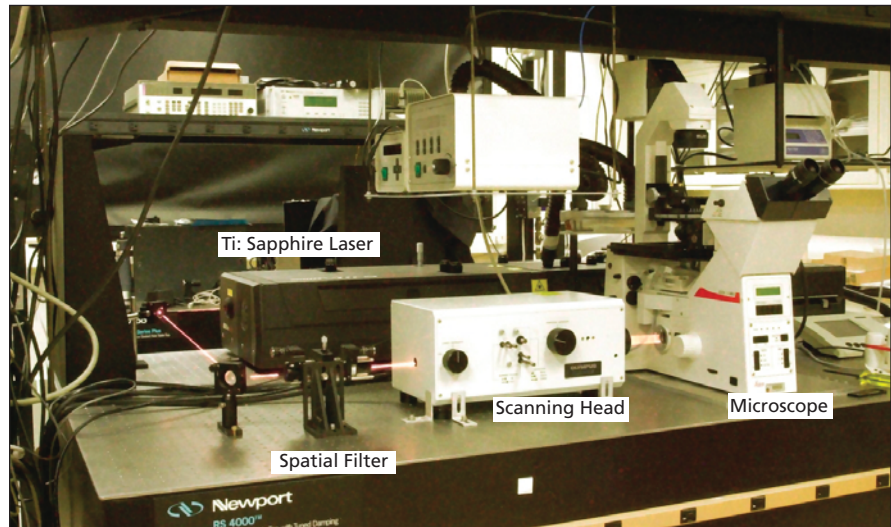


Figure 1. This Optoelectronic System is a custom-built system for two-photon fluorescence microscopy.

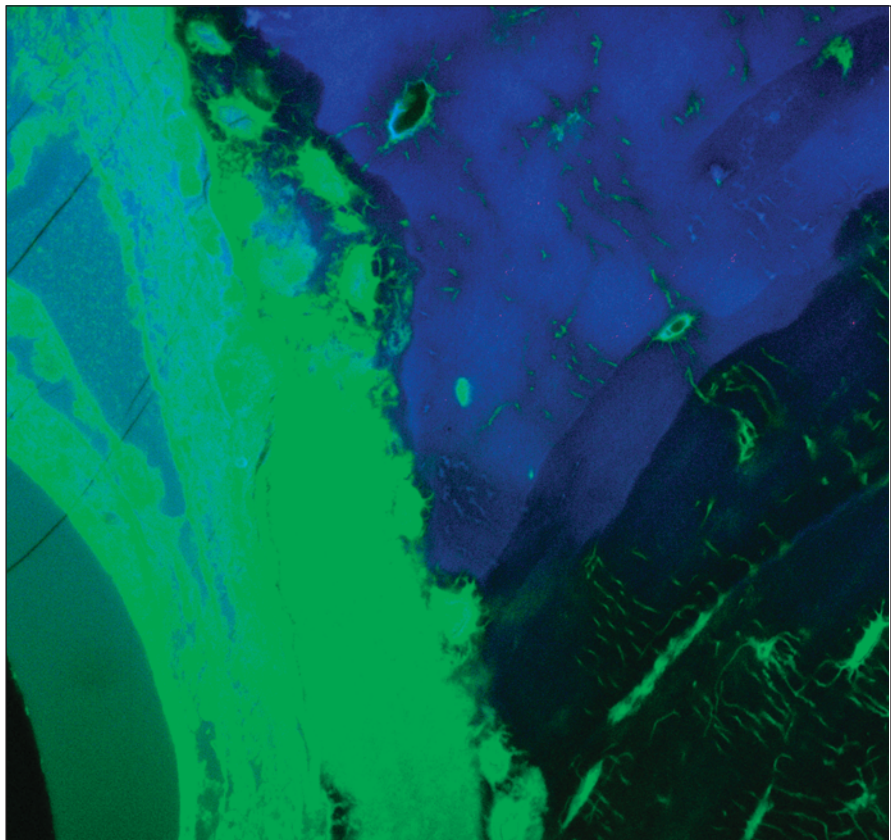


Figure 2. This Two-Photon Image of a human femur section shows several areas of remodeled bone. The field of view is 200 μm . The specimen in this image was provided by the Cleveland Clinic Foundation.

Center and Marius Asipauskas of the National Center for Microgravity Research.

Inquiries concerning rights for the commercial use of this invention should be addressed

to NASA Glenn Research Center, Commercial Technology Office, Attn: Steve Fedor, Mail Stop 4-8, 21000 Brookpark Road, Cleveland, Ohio 44135. Refer to LEW-17573-1.



▶ Biased Randomized Algorithm for Fast Model-Based Diagnosis

The bias increases the likelihood of making a minimal diagnosis.

NASA's Jet Propulsion Laboratory, Pasadena, California

A biased randomized algorithm has been developed to enable the rapid computational solution of a propositional-satisfiability (SAT) problem equivalent to a diagnosis problem. The closest competing methods of automated diagnosis are described in the preceding article "Fast Algorithms for Model-Based Diagnosis" and "Two Methods of Efficient Solution of the Hitting-Set Problem" (NPO-30584), which appears elsewhere in this issue.

It is necessary to recapitulate some of the information from the cited articles as a prerequisite to a description of the present method. As used here, "diagnosis" signifies, more precisely, a type of model-based diagnosis in which one explores any logical inconsistencies between the observed and expected behaviors of an engineering system. The function of each component and the interconnections among all the components of the engineering system are represented as a logical system. Hence, the expected behavior of the engineering system is represented as a set of logical consequences. Faulty components lead to inconsistency between the observed and expected behaviors of the system, represented by logical inconsistencies. Diagnosis — the task of finding the faulty components — reduces to finding the components, the abnormalities of which could explain all the logical inconsisten-

cies. One seeks a minimal set of faulty components (denoted a minimal diagnosis), because the trivial solution, in which all components are deemed to be faulty, always explains all inconsistencies.

In the methods of the cited articles, the minimal-diagnosis problem is treated as equivalent to a minimal-hitting-set problem, which is translated from a combinatorial to a computational problem by mapping it onto the Boolean-satisfiability and integer-programming problems. The integer-programming approach taken in one of the prior methods is complete (in the sense that it is guaranteed to find a solution if one exists) and slow and yields a lower bound on the size of the minimal diagnosis. In contrast, the present approach is incomplete and fast and yields an upper bound on the size of the minimal diagnosis.

The encoding of the diagnosis problem as an SAT problem for the purpose of the present method is basically the same as the encoding of the diagnosis problem as a hitting-set problem in the methods of the cited articles. In the present case, one seeks a minimal solution to the SAT problem — that is, a solution in which the fewest variables are set to TRUE. In a typical prior local-search algorithm for solving the SAT problem, one guesses at a complete solution and then, through a sequence of partly random and partly greedy flips,

tries to adjust the guess to reduce the number of unsatisfied clauses while increasing, or leaving unchanged, the number of satisfied clauses. Eventually, one converges toward a complete solution. Although such local-search algorithms are not complete, in practice, they outperform other algorithms for solving the SAT problem.

The prior local-search algorithms used to solve the SAT problem sometimes flounder in the search space without converging to the solution, making it necessary to restart the algorithms from time to time. Usually, in such a case, one randomly assigns a value of TRUE or FALSE to each variable in the SAT problem. In the present algorithm, one biases this otherwise random assignment toward FALSE in the effort to make the subsequent random and greedy flips lead to a solution in which the fewest variables are TRUE. Hence, one increases the probability of reaching a minimal solution. If the solution is not a minimal diagnosis, it is nevertheless guaranteed to provide an upper bound on the minimal diagnosis, and thereby to be useful as a guide to the use of other diagnostic algorithms.

This work was done by Colin Williams and Farrokh Vartan of Caltech for NASA's Jet Propulsion Laboratory. Further information is contained in a TSP (see page 1). NPO-40065

▶ Fast Algorithms for Model-Based Diagnosis

Methods based on Boolean functions and linear programming are more practical for complex systems.

NASA's Jet Propulsion Laboratory, Pasadena, California

Two improved new methods for automated diagnosis of complex engineering systems involve the use of novel algorithms that are more efficient than prior algorithms used for the same purpose. Both the recently developed algorithms and the prior algorithms in question are instances of model-based diagnosis, which is based on exploring the logical inconsis-

tency between an observation and a description of a system to be diagnosed.

As engineering systems grow more complex and increasingly autonomous in their functions, the need for automated diagnosis increases concomitantly. In model-based diagnosis, the function of each component and the interconnections among all the components of the sys-

tem to be diagnosed (for example, see figure) are represented as a logical system, called the system description (SD). Hence, the expected behavior of the system is the set of logical consequences of the SD. Faulty components lead to inconsistency between the observed behaviors of the system and the SD. The task of finding the faulty components (diagnosis) re-

duces to finding the components, the abnormalities of which could explain all the inconsistencies. Of course, the meaningful solution should be a minimal set of faulty components (called a minimal diagnosis), because the trivial solution, in which all components are assumed to be faulty, always explains all inconsistencies. Although the prior algorithms in question implement powerful methods of diagnosis, they are not practical because they essentially require exhaustive searches among all possible combinations of faulty components and therefore entail the amounts of computation that grow exponentially with the number of components of the system.

For the purpose of establishing the basis of an algorithmic approach that entails more efficient computation, and, more specifically, translating the

diagnosis problem from a logical problem to a computational problem, it was shown that the calculation of minimal diagnosis can be mapped as the solution of two well-known problems — the Boolean satisfiability and the integer-programming. The first new method is based on the connection between the diagnosis problem and the Boolean satisfiability problem. This connection makes it possible to use Boolean function theory to reduce the diagnosis problem to the problem of finding prime-implicants (which is one of the basic problems in the theory of Boolean functions). This, in turn, makes it possible to utilize powerful and efficient algorithms, recently developed for the satisfiability problem, to compute the minimal diagnosis. The algorithm thus developed to solve the diagnosis prob-

lem requires an amount of computation proportional to a superpolynomial function of n (meaning that the computation time is proportional to $n^{\log n}$), where n is the number of components of the system.

The second new method is based on the mapping of the diagnosis problem onto the integer-programming problem. This mapping makes it possible to utilize the large and versatile body of computational techniques developed previously for linear integer programming optimization to solve the diagnosis problem in an approach more practical than that of the prior exhaustive-search algorithms. Some of the integer programming techniques, modified to make them suitable for solving the diagnosis problem, can efficiently diagnose a system that contains as many as several thousand components.

This work was done by Amir Fijany, Anthony Barrett, Farrokh Vatan, and Ryan Mackey of Caltech for NASA's Jet Propulsion Laboratory. Further information is contained in a TSP (see page 1).

In accordance with Public Law 96-517, the contractor has elected to retain title to this invention. Inquiries concerning rights for its commercial use should be addressed to:

*Innovative Technology Assets Management
JPL*

Mail Stop 202-233

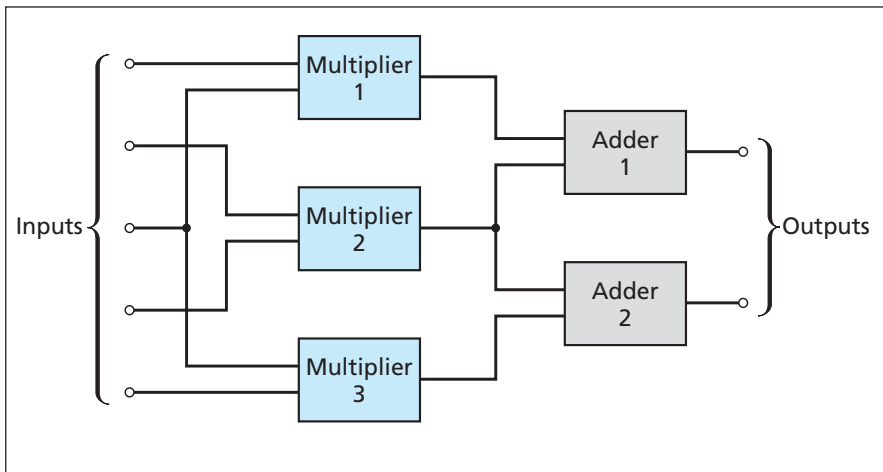
4800 Oak Grove Drive

Pasadena, CA 91109-8099

(818) 354-2240

E-mail: iaoffice@jpl.nasa.gov

Refer to NPO-30582, volume and number of this NASA Tech Briefs issue, and the page number.



This Network of Multipliers and Adders is a relatively simple example of an engineering system amenable to model-based diagnosis.



Simulations of Evaporating Multicomponent Fuel Drops

A paper presents additional information on the subject matter of “Model of Mixing Layer With Multicomponent Evaporating Drops” (NPO-30505), *NASA Tech Briefs*, Vol. 28, No. 3 (March 2004), page 55. To recapitulate: A mathematical model of a three-dimensional mixing layer laden with evaporating fuel drops composed of many chemical species has been derived. The model is used to perform direct numerical simulations in continuing studies directed toward understanding the behaviors of sprays of liquid petroleum fuels in furnaces, industrial combustors, and engines. The model includes governing equations formulated in an Eulerian and a Lagrangian reference frame for the gas and drops, respectively, and incorporates a concept of continuous thermodynamics, according to which the chemical composition of a fuel is described by use of a distribution function. In this investigation, the distribution function depends solely on the species molar weight. The present paper reiterates the description of the model and discusses further in-depth analysis of the previous results as well as results of additional numerical simulations assessing the effect of the mass loading. The paper reiterates the conclusions reported in the cited previous article, and states some new conclusions. Some new conclusions are:

1. The slower evaporation and the evaporation/condensation process for multicomponent-fuel drops resulted in a reduced drop-size polydispersity compared to their single-component counterpart.
2. The inhomogeneity in the spatial distribution of the species in the layer increases with the initial mass loading.
3. As evaporation becomes faster, the assumed invariant form of the molecular-weight distribution during evaporation becomes inaccurate.

*This work was done by Josette Bellan and Patrick Le Clercq of Caltech for NASA’s Jet Propulsion Laboratory. Further information is contained in a TSP (see page 1).
NPO-30641*

Formation Flying of Tethered and Nontethered Spacecraft

A paper discusses the effect of the dynamic interaction taking place within a formation composed of a rigid and a deformable vehicle, and presents the concept of two or more tethered spacecraft flying in formation with one or more separated free-flying spacecraft. Although progress toward formation flight of nontethered spacecraft has already been achieved, the document cites potential advantages of tethering, including less consumption of fuel to maintain formation, very high dynamic stability of a rotating tethered formation, and intrinsically passive gravity-gradient stabilization. The document presents a theoretical analysis of the dynamics of a system comprising one free-flying spacecraft and two tethered spacecraft in orbit, as a prototype of more complex systems. The spacecraft are modeled as rigid bodies and the tether as a mass-less spring with structural viscous damping. Included in the analysis is a study of the feasibility of a centralized control system for maintaining a required formation in low Earth orbit. A numerical simulation of a retargeting maneuver is reported to show that even if the additional internal dynamics of the system caused by flexibility is considered, high pointing precision can be achieved if a fictitious rigid frame is used to track the tethered system, and it should be possible to position the spacecraft with centimeter accuracy and to orient the formation within arc seconds of the desired direction also in the presence of low Earth orbit environmental perturbations. The results of the study demonstrate that the concept is feasible in Earth orbit and point the way to further study of these hybrid tethered and free-flying systems for related applications in orbit around other Solar System bodies.

*This work was done by Marco B. Quadrelli of Caltech for NASA’s Jet Propulsion Laboratory. Further information is contained in a TSP (see page 1).
NPO-30730*

Two Methods for Efficient Solution of the Hitting-Set Problem

A paper addresses much of the same subject matter as that of “Fast Algorithms for Model-Based Diagnosis” (NPO-30582), which appears elsewhere in this issue of *NASA Tech Briefs*. However, in the paper, the emphasis is more on the hitting-set problem (also known as the transversal problem), which is well known among experts in combinatorics. The authors’ primary interest in the hitting-set problem lies in its connection to the diagnosis problem: it is a theorem of model-based diagnosis that in the set-theory representation of the components of a system, the minimal diagnoses of a system are the minimal hitting sets of the system. In the paper, the hitting-set problem (and, hence, the diagnosis problem) is translated from a combinatorial to a computational problem by mapping it onto the Boolean satisfiability and integer-programming problems. The paper goes on to describe developments nearly identical to those summarized in the cited companion *NASA Tech Briefs* article, including the utilization of Boolean-satisfiability and integer-programming techniques to reduce the computation time and/or memory needed to solve the hitting-set problem.

This work was done by Farrokh Vatan and Amir Fijany of Caltech for NASA’s Jet Propulsion Laboratory. Further information is contained in a TSP (see page 1).

In accordance with Public Law 96-517, the contractor has elected to retain title to this invention. Inquiries concerning rights for its commercial use should be addressed to:

*Innovative Technology Assets Management
JPL*

*Mail Stop 202-233
4800 Oak Grove Drive
Pasadena, CA 91109-8099
(818) 354-2240*

E-mail: iaoffice@jpl.nasa.gov

Refer to NPO-30584, volume and number of this NASA Tech Briefs issue, and the page number.



National Aeronautics and
Space Administration